63-3-12

PR-63-1

PROGRESS REPORT
RADIATION RESISTANT ELECTRONICS

by O.L. Meyer,
J.L. Scales
and others
~~C.H. Klute~~
~~H. Morris~~

1 July 1962 to 31 December 1962

HARRY DIAMOND LABORATORIES
FORMERLY: DIAMOND ORDNANCE FUZE LABORATORIES
ARMY MATERIEL COMMAND
WASHINGTON 25, D. C.

F 4.60

HARRY DIAMOND LABORATORIES

Robert W. McEvoy
LtCol, Ord Corps
Commanding

B. M. Horton
Technical Director

MISSION

The mission of the Harry Diamond Laboratories is:

(1) To perform research and engineering on systems for detecting, locating, and evaluating targets; for accomplishing safing, arming, and munition control functions; and for providing initiation signals: these systems include, but are not limited to, radio and non-radio proximity fuzes, predictor-computer fuzes, electronic timers, electrically-initiated fuzes, and related items.

(2) To perform research and engineering in fluid amplification and fluid-actuated control systems.

(3) To perform research and engineering in instrumentation and measurement in support of the above.

(4) To perform research and engineering in order to achieve maximum immunity of systems to adverse influences, including countermeasures, nuclear radiation, battlefield conditions, and high-altitude and space environments.

(5) To perform research and engineering on materials, components, and subsystems in support of above.

(6) To conduct basic research in the physical sciences in support of the above.

(7) To provide consultative services to other Government agencies when requested.

(8) To carry out special projects lying within installation competence upon approval by the Director of Research and Development, Army Materiel Command.

(9) To maintain a high degree of competence in the application of the physical sciences to the solution of military problems.

(5) 391 950

UNITED STATES ARMY MATERIEL COMMAND
HARRY DIAMOND LABORATORIES
WASHINGTON 25, D.C.

NAS-W-251
OMS Code 5010.21.83701
HDL Proj 94892

(4) (Rept. no. PR-63-1)

(7) PROGRESS REPORT

(6) RADIATION RESISTANT ELECTRONICS

1 July ~~1962~~ to 31 Dec~~ember 1962~~

For (8) See Front cover

(9) 31 Dec 62

(10) 45p. incl. illus. 28 refs.

(12) NA

(13) NA

FOR THE COMMANDER:
Approved by

P. E. Landis
Chief, Laboratory 900

NASA Defense Purchase Request No. GMS-84

CONTENTS

ABSTRACT

This is the third semiannual progress report on a program to develop radiation-resistant electronics. The program is managed by the Harry Diamond Laboratories (formerly the Diamond Ordnance Fuze Laboratories) with the support of the National Aeronautics and Space Administration. In addition to in-house work at HDL, contracts have been let with the Philco Corporation to develop thin-film active devices and with the General Electric Company for work on tunneling cathodes. The contractors will submit individual quarterly progress reports.

During the period covered by this report, a more detailed theoretical study has been made of the field emission process in thin-film devices than was made earlier. It was demonstrated in one example that increasing the dielectric constant of the emitter-base insulating layer from 1 to 3 could be expected to reduce the internal field emission current by two orders of magnitude. Improvements in the yield of functioning aluminum-aluminum oxide-aluminum tunneling sandwiches were realized when such sandwiches were overcoated with silicon monoxide, just after preparation. The experiment of Kahng, in which a mercury emitter electrode was used to establish the existence of hot electrons in thin-film active devices, was conducted with the objective being to duplicate Kahng's results and expand on his work by operating the device as an amplifier. Triode action was observed, but there was no voltage or power gain. A new technique was investigated for the fabrication of metal-interface amplifiers which was intended to completely eliminate the effect of pinholes in the insulating layer of these devices. This technique was not, however, successful. A number of improvements in laboratory instrumentation incident to this work are also described.

1. INTRODUCTION

This is the third semiannual progress report describing work on radiation-resistant electronics, which is supported by the National Aeronautics and Space Administration. The program consists of an in-house effort at the Harry Diamond Laboratories (formerly the Diamond Ordnance Fuze Laboratories) and two contracted programs, one at the Philco Corporation and another at the General Electric Company. The program has as its goal the development of radiation resistant devices utilizing tunneling or other conduction phenomena in thin-film structures.

2. PROGRESS—THEORETICAL

In the first of this series of progress reports (ref 1) an examination of the emission process in metal-insulator-metal sandwiches was made which considered only the tunneling process in an elementary way and excluded all other effects that might have been occurring simultaneously. In the following section of this report the emission problem is re-examined using a more advanced theoretical treatment. The mathematics of this treatment becomes very involved; accordingly an abbreviated account is given here which is

intended to hit the high spots of the research as well as to indicate the conclusions that may be drawn at present. A detailed account of the emission problem will be the subject of a separate report.

2.1 Analysis of Field Emission According to the Theory of Murphy and Good

Calculations were performed to give the current-voltage characteristics of a three-layer diode of the type consisting of a metal-insulator-metal sandwich. The basis of the calculations was the theory of Murphy and Good (ref 2) originally developed to explain field emission from a metal into vacuum. In order to use this theory it is necessary to argue that replacing the vacuum with an insulating material does not change the problem significantly. This can be done plausibly provided one is willing to permit a broad conduction band in the insulator so that—although most electrons cannot propagate—the few with sufficient energy to do so, propagate freely.

Electrons can enter the insulator by going over the top of the potential barrier (see fig. 1) or by tunneling through the barrier. The total current is determined by integrating over all energies, the product of the electronic charge q, the electron flux N(W), and transmission probability D(W).

$$J = -q \int_0^{\infty} N(W)\, D(W)\, dW \tag{1}$$

At high energies, D(W) is unity and the current is determined by N(W), which is very small. This is the ordinary thermionic emission problem. At energies below the Fermi energy, the electron flux N(W) is large but the transmission coefficient D(W) is small. This is the tunneling problem treated by Holm (ref 3). There is an energy interval, higher than the Fermi energy but below the height of the barrier, where N(W) and D(W) are of comparable magnitude. This region makes the dominant contribution to the current. The analysis of Murphy and Good was preferred to that of Holm, because it was more accurate in this critical region and included a better treatment of image forces than did the latter.

Murphy and Good write their equations in terms of dimensionless variables. For example, ϕ represents the barrier height divided by a characteristic energy, F represents electric field divided by a characteristic field, etc. The characteristic field, current density and energy unit are listed below:

$$F_o = m_o^2\, q^5/\hbar^4 = 5.15 \times 10^9 \text{ v/cm} \tag{2a}$$

$$J_o = m_o^3\, q^9/\hbar^7 = 2.37 \times 10^{14} \text{ amp/cm}^2 \tag{2b}$$

$$W_o = m_o\, q^4/\hbar^3 = 27.2 \text{ ev} \tag{2c}$$

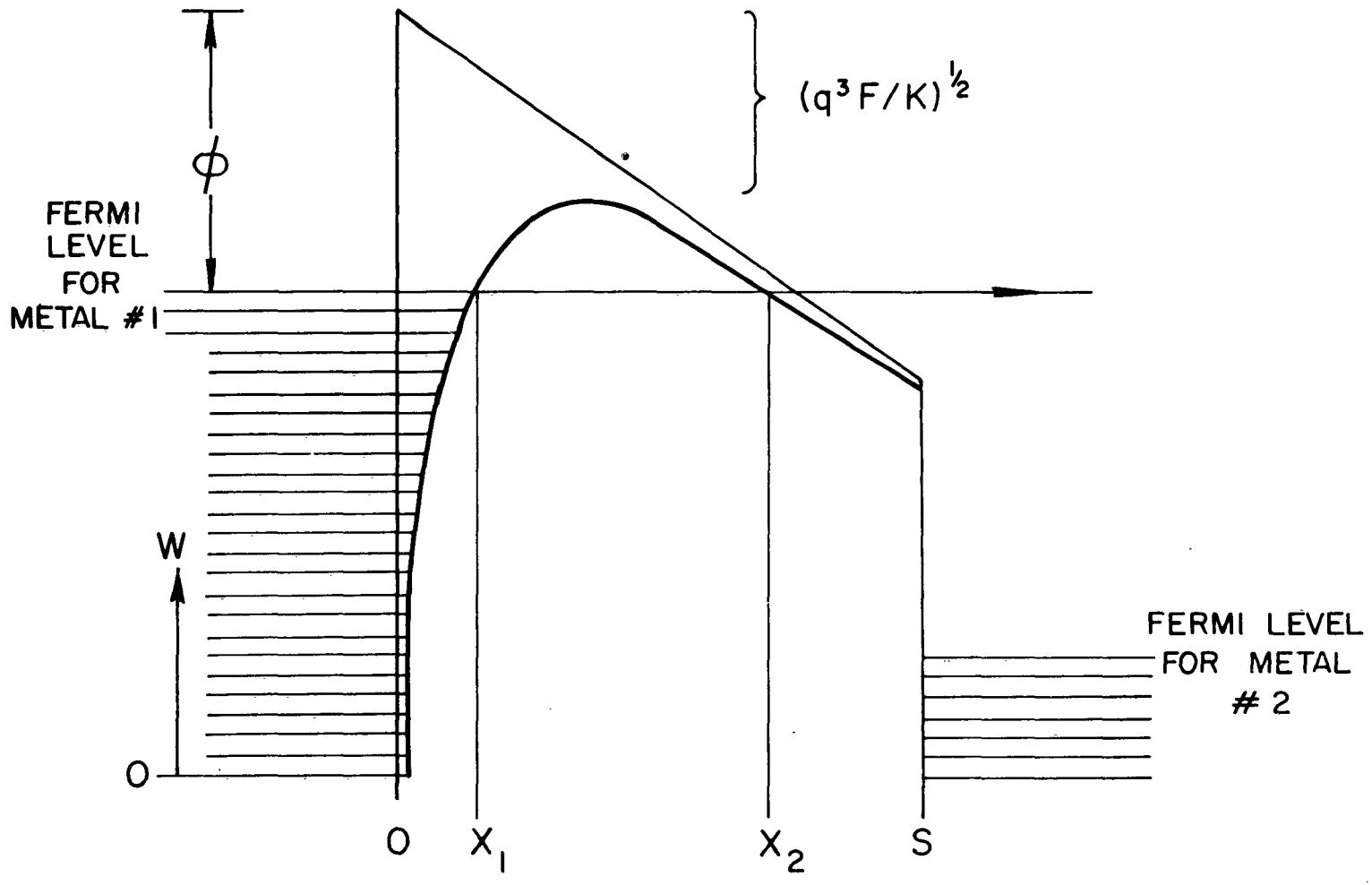

Figure 1. Energy level diagram for field emission in a thin film diode.

where

m_o = mass of an electron in vacuum

q = electronic charge

$\hbar$ = Planck's constant divided by 2π

There are two expressions for the current; one is valid at low fields and the other at high fields.

At low fields the current density is

$$J = \frac{1}{2}\left(\frac{kT}{\pi}\right)^2 \left(\frac{m}{m_o}\right) \frac{\pi d}{\sin \pi d} \exp\left(-\frac{\phi - D}{kT}\right) \tag{3}$$

where

$$d = K^{1/4}\left(\frac{m_o}{M}\right)^{1/2}\left(\frac{F^{3/4}}{\pi kT}\right) \tag{4a}$$

and

$$D = (q^3 F/K)^{1/2} \tag{4b}$$

In these equations,

m = effective mass of an electron in a metal

M = effective mass of an electron in the insulator

K = relative dielectric constant of the insulator

Note that as $d \to 0$, equation (3) passes over into the Richardson-Schottky expression for thermionic emission over a reduced barrier. Equation 3 is valid provided two conditions are satisfied:

$$(1) \quad \ell n\left(\frac{1-d}{d}\right) - \frac{1}{1-d} > -\frac{\pi}{F^{1/2}} \tag{5}$$

$$(2) \quad d\ \ell n\left(\frac{1-d}{d}\right) - \frac{1}{1-d} > -\left(\frac{\phi - D}{kT}\right) \tag{6}$$

At room temperature, assuming the values $M = 0.5\ m_o$ and $K = 3$, the first equation requires that the field be less than 1.8×10^6 v/cm. The second condition brings in a relation between field and barrier height. It is more restrictive than the first condition if the barrier height is less than 0.7 ev.

At high fields the current is given by the expression

$$J = \left(\frac{m m_o}{M^2}\right) \frac{F^2}{16\pi^3 \phi\, t^2} \frac{\pi\, ckT}{\sin \pi\, ckT} \exp\left[-\frac{4\sqrt{2}\,\phi^{3/2}\, v}{3F}\right] \tag{7}$$

where t, c, v and f are functions of the variable $(F^{1/2}/\phi K^{1/2})$. These functions are defined in ref 2 . There are two conditions of validity:

$$(1) \quad 1 - ckT > kT\sqrt{2f} \tag{8}$$

$$(2) \quad (\phi^{1/2} - F) > \frac{F^{3/4}}{\pi} + \frac{kT}{1-ckT} \tag{9}$$

The first condition requires that the field be larger than some threshold. The second condition requires that the field be less than some limiting value.

Figure 2 shows curves of current density versus field, for different actual barrier heights. The curves were computed from equation 7, assuming $m = M = m_o$ and $K = 1$. A change of 0.1 v in the height of the barrier causes about an order of magnitude change in the current. Figure 3 illustrates the effect of dielectric constant. Changing from $K = 1$ to $K = 3$ causes about two orders of magnitude reduction in the current.

The analysis thus far takes no account of the fact that a second metal is in contact with the insulator. To get the net current through the insulator, one must subtract the emission from the second metal to the first metal. In this reverse problem, the barrier has the same shape (i.e. the same electric field present) but the apparent work function is $(\phi + qV)$ instead of ϕ. The second metal is assumed to be at a positive potential V, which is equivalent to lowering the Fermi level (and all electron energies) by an amount qV (in esu units). Therefore, to get the net current, one must compute the quantity:

$$J_{net} = J(\phi,F) - J(\phi+qV,F) \tag{10}$$

where, at each value of F, the potential is given by $V = Fs$ where s is the thickness of the insulator. It is apparent from figures 2 and 3 that a small increase in barrier height causes a large reduction in the tunneling current. Therefore the second term in equation 10 will be much smaller than the first term and will usually be negligible, except for very weak fields.

3. PROGRESS—EXPERIMENTAL

In the following sections, an account is given of the results of the experimental activities pursued during the period reported. In almost every case the experimental work proceeded along the lines laid out in the preceding progress report.

3.1 Vacuum Technology

A new vacuum evaporator, shown in figure 4 was received and put into operation. The performance of this equipment is now satisfactory after a considerable time spent in checking it out, tracing leaks, and making

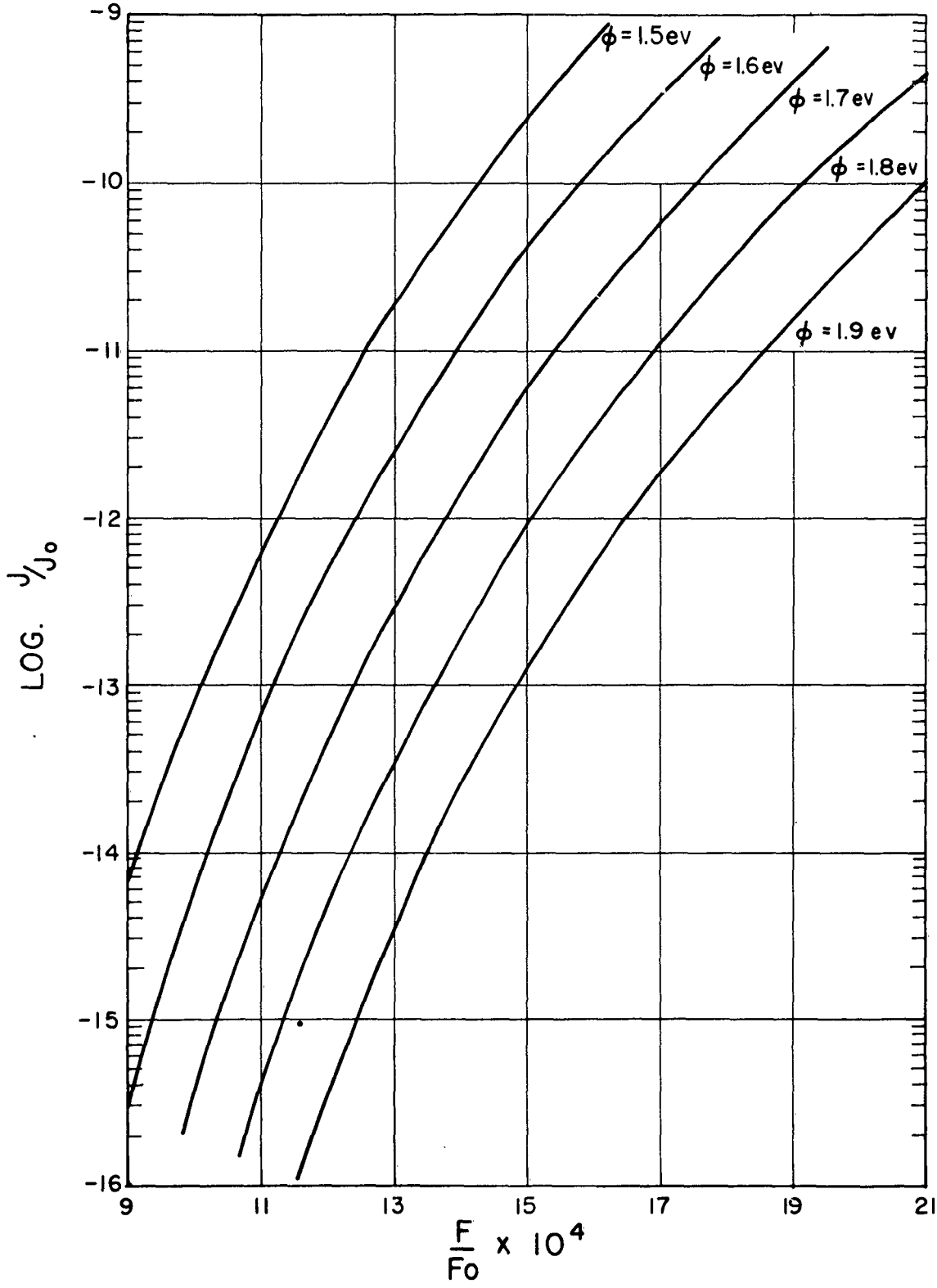

Figure 2. Relative current density as a function of relative field strength for various actual barrier heights.

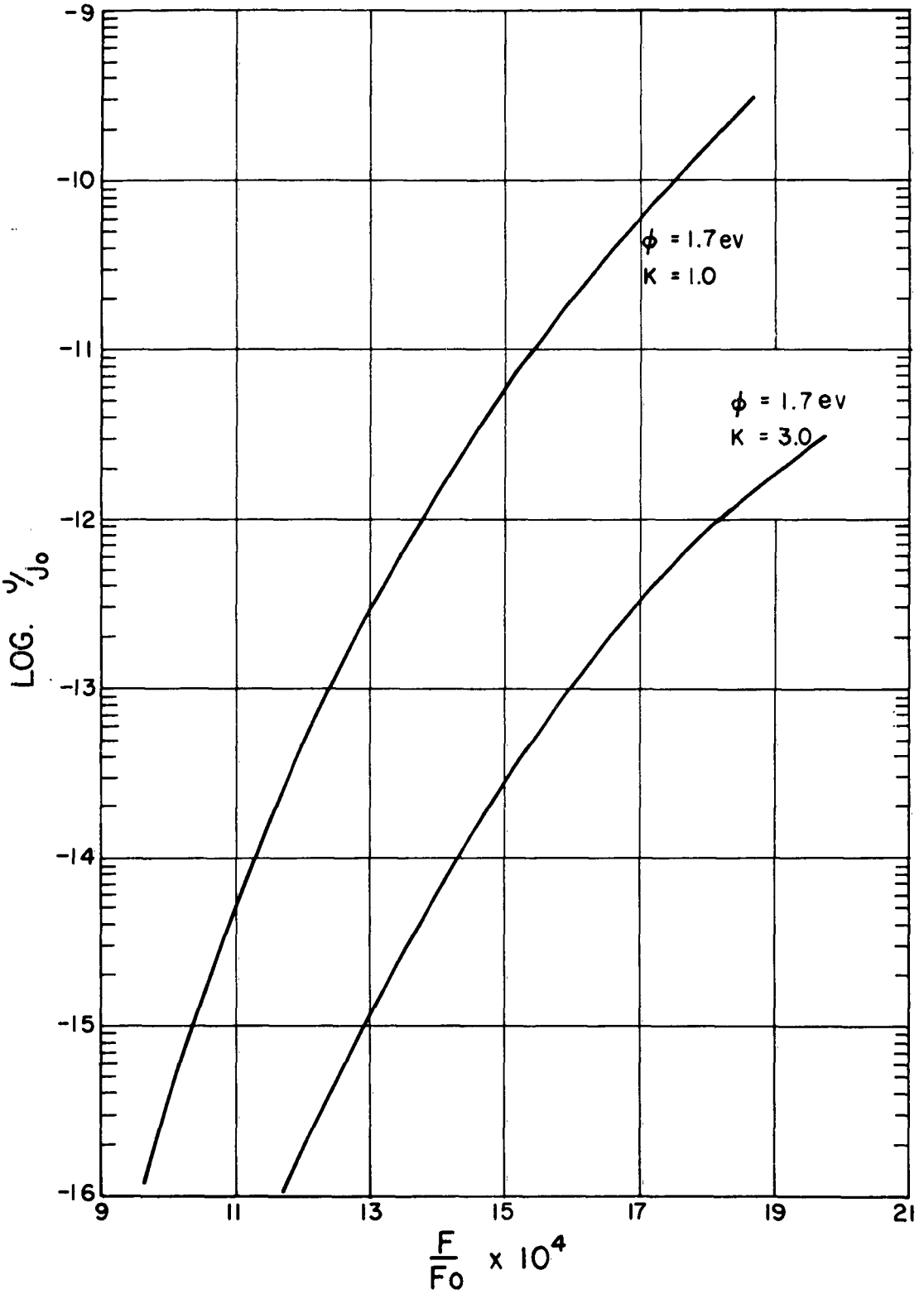

Figure 3. Relative current density as a function of relative field strength for relative dielectric constants of 1 and 3.

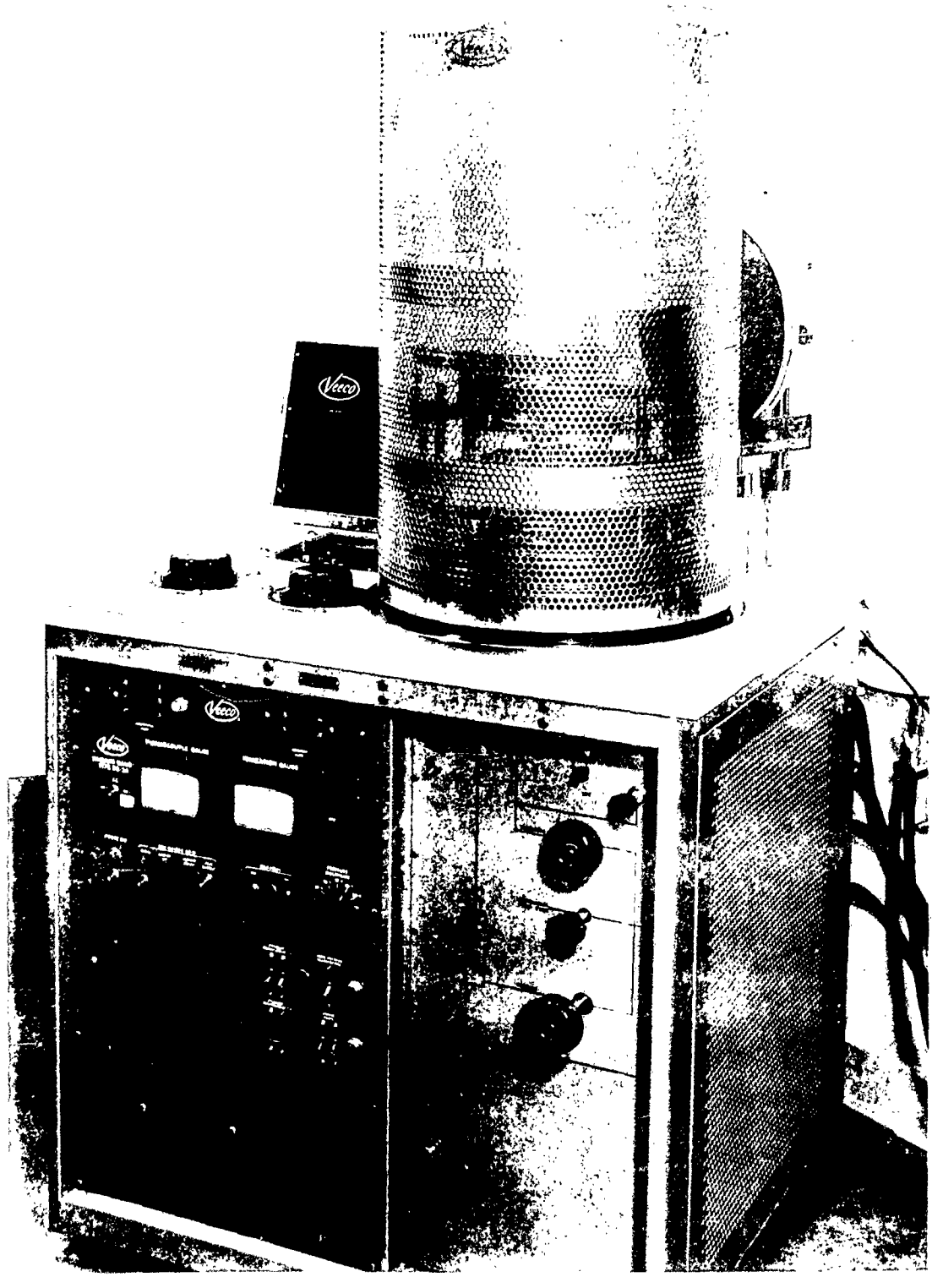

Figure 4. Recently acquired high vacuum system. 167-63

modifications. The major leak was found to be the atmosphere inlet valve, with the trouble being caused by dust particles that had been sucked in and deposited on the teflon valve seat when the bell jar was vented. The system was modified by the installation of the Meissner trap (shown in fig. 5), the conversion to fluorocarbon elastomer O-rings, and the conversion to silicone oil in the diffusion pump. The bell jar hoist was also modified to enable the bell jar to be rotated in the elevated position and thus be cleaned conveniently and thoroughly. As a result of the modifications, and the elimination of leaks, a pressure of 5.5×10^{-8} Torr was achieved in the 18 in. by 30 in. bell jar in less than 2 hr without baking.

Specifications were written and submitted for the purchase of an ultra-high-vacuum evaporator with ion pumps.

Some modifications were made on a laboratory-assembled vacuum system, intended for use as an experimental system for developing both advanced vacuum and evaporation techniques. A 14-in. diameter base plate with filament power feed-throughs was installed. A leak was found in one of the O-rings. This was corrected and the system is being checked to determine ultimate pressures obtainable.

3.2 Triode Structures

Two types of thin-film active triodes were the subject of separate experiments during the report period, viz: the metal edge amplifier and the device reported by Kahng during 1962. The first of these is not a hot electron device whereas the second is.

Attempts were made to fabricate an MEA device or "metal edge amplifier" on low-resistivity n-type silicon. The objective of these particular experiments was to fabricate such a device without the use of overlapping films, and thus eliminate the problem of pin holes and short circuits. It is the practice of other workers in this field (ref 4 and 5) to fabricate MEA devices on germanium by vacuum depositing an aluminum film thereon, growing an oxide on the film under controlled conditions, and then depositing a second film of aluminum that slightly overlaps one edge of the first. The result is a structure as shown in figure 6, where two surface barrier junctions are formed on the germanium separated by the thickness of the oxide film. When the diodes are both reverse biased, and when a bias also exists between the aluminum films, but remains small enough so that the insulating film is not broken down, a high field exists between the metal films and fringes into the semiconductor. The high field causes a Zener or avalanche breakdown in the depletion region, and this, in turn, provides copious quantities of electrons for collection in the bulk germanium.

In the HDL work with silicon, the objective was to locate two areas of vacuum-deposited gold film on the surface of the silicon, so that the surface barrier junctions thus formed are separated by a distance of about 50 Å. The principle of the fabrication technique employed was to

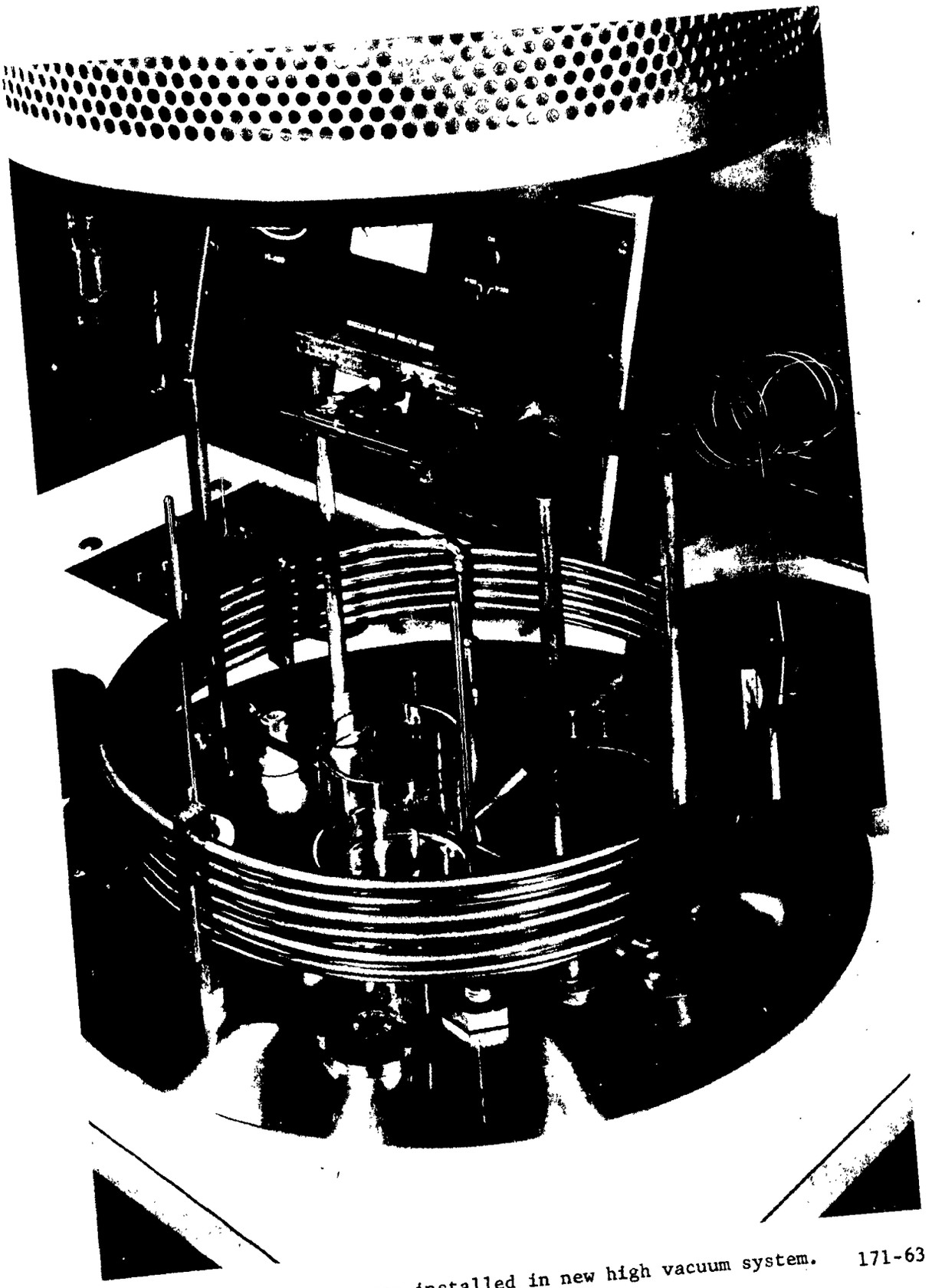

Figure 5. Meissner trap installed in new high vacuum system. 171-63

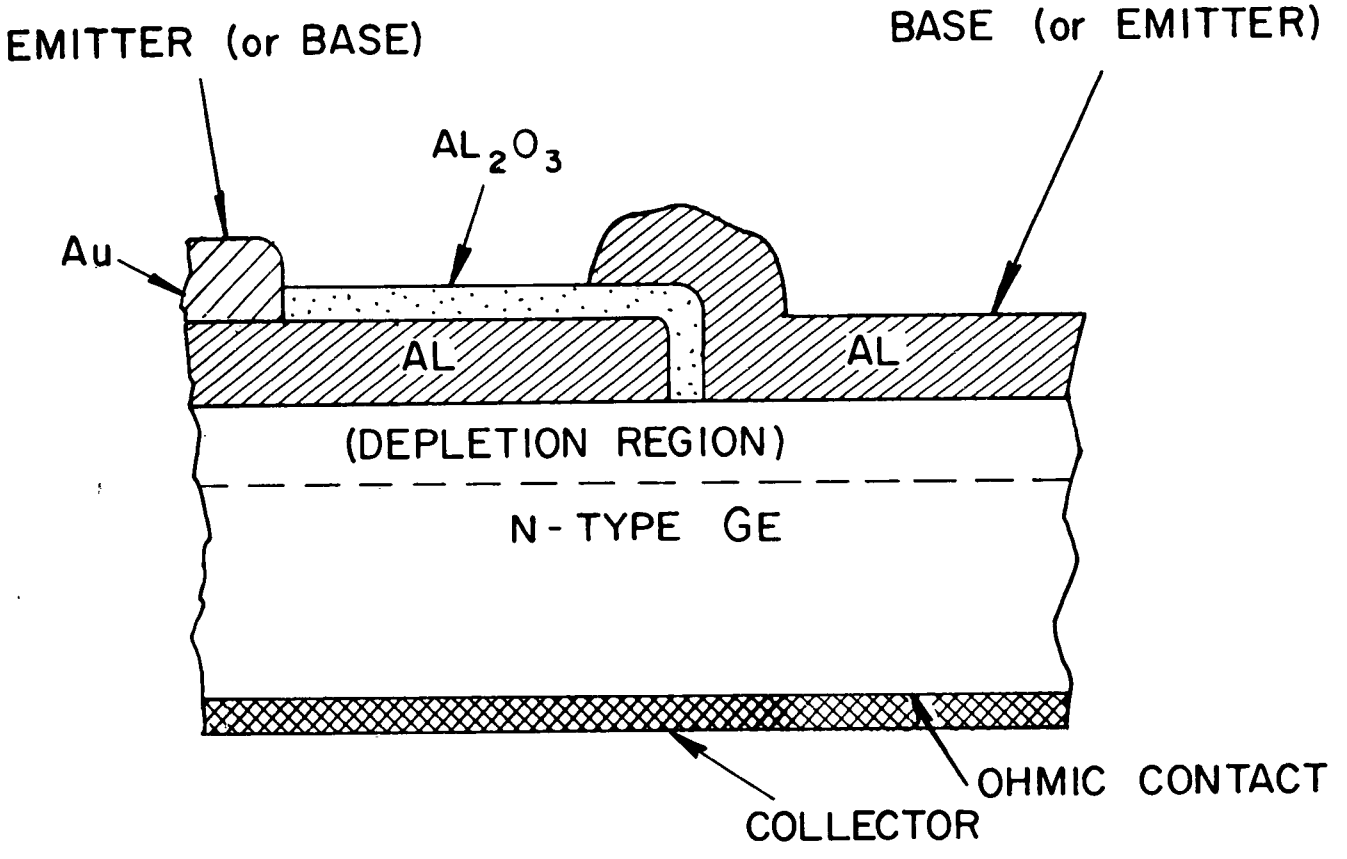

Figure 6. Conventional structure of the metal edge amplifier.

make use of silicon-oxide masking and deposit the metal film at an angle such that it was shadowed or masked by a sharp step on the surface of the wafer as shown in figure 7. One of the techniques employed was to form a step of known height (300 Å) on the surface of the silicon. The procedure used was to cover part of the silicon wafer surface with silicon oxide film about 7000 A thick. The oxide was then regrown on the uncovered area to a depth sufficient to form a 300-Å step in the surface of the silicon wafer. The step was subsequently exposed by removing all the oxide with a hydrofluoric acid etch. Gold was then deposited at an angle such that the step masked the deposition as described previously. This technique proved unsuccessful in several devices due to electrical shorts between the areas of gold film. Another method tried involved the same principle of masking the gold deposition, but substituted the sharp edge of a gold film, deposited previously, for the step in the silicon. The problem here was to obtain a step edge to the first gold deposition. Attempts were made to do so by masking with an oxide film, photosensitive lacquer, and wax, but all these techniques were unsuccessful. Both of these procedures are predicated upon the assumption that the surface mobility of gold on silicon would be a factor Thus if this mobility were low (sharp shadowing) the second device should be favored. If the mobility were high (diffuse shadowing) the first mentioned device would be favored. Actually the results indicate that under the conditions of the experiment either the mobility was so high, and/or the geometry of the step so deficient, that the electrodes were short-circuited in both cases.

Although the results of those experiments were disappointing, they do not rule out the possibility that a superior MEA could be made this way. However, this line of experimentation was considered less important than other planned work; accordingly it was dropped for the present.

Kahng's experiments with thin-film tunneling devices provide powerful support for the thesis that hot electrons are indeed generated in these structures, as opposed to a depletion layer mechanism of operation involving pinholes (ref 5, 6). Accordingly it seemed desirable to repeat these experiments at HDL. The experiments were conducted using a device structure consisting of a polished wafer of low-resistivity n-type silicon on which a 100-Å layer of gold had been vacuum deposited to form a surface barrier junction. The gold base layer was then overcoated with a vacuum-deposited insulating film of silicon monoxide, 40 Å thick. A mercury electrode served as the emitter and was brought into contact with the insulating film of silicon monoxide. The argument underlying the experiment is that the mercury will amalgamate the base metal (i.e. gold) and destroy the device where pinholes exist in the oxide layer. Where pinholes do not exist, the device must function as a hot electron device, if it is to function at all. Several of these devices were made in the manner described. One of them, with the mercury emitter electrode in contact with the insulating film is shown in figure 8. In some of these devices, triode action was indeed observed as reported by Kahng. Characteristic curves shown in figure 9 demonstrate that the alpha observed

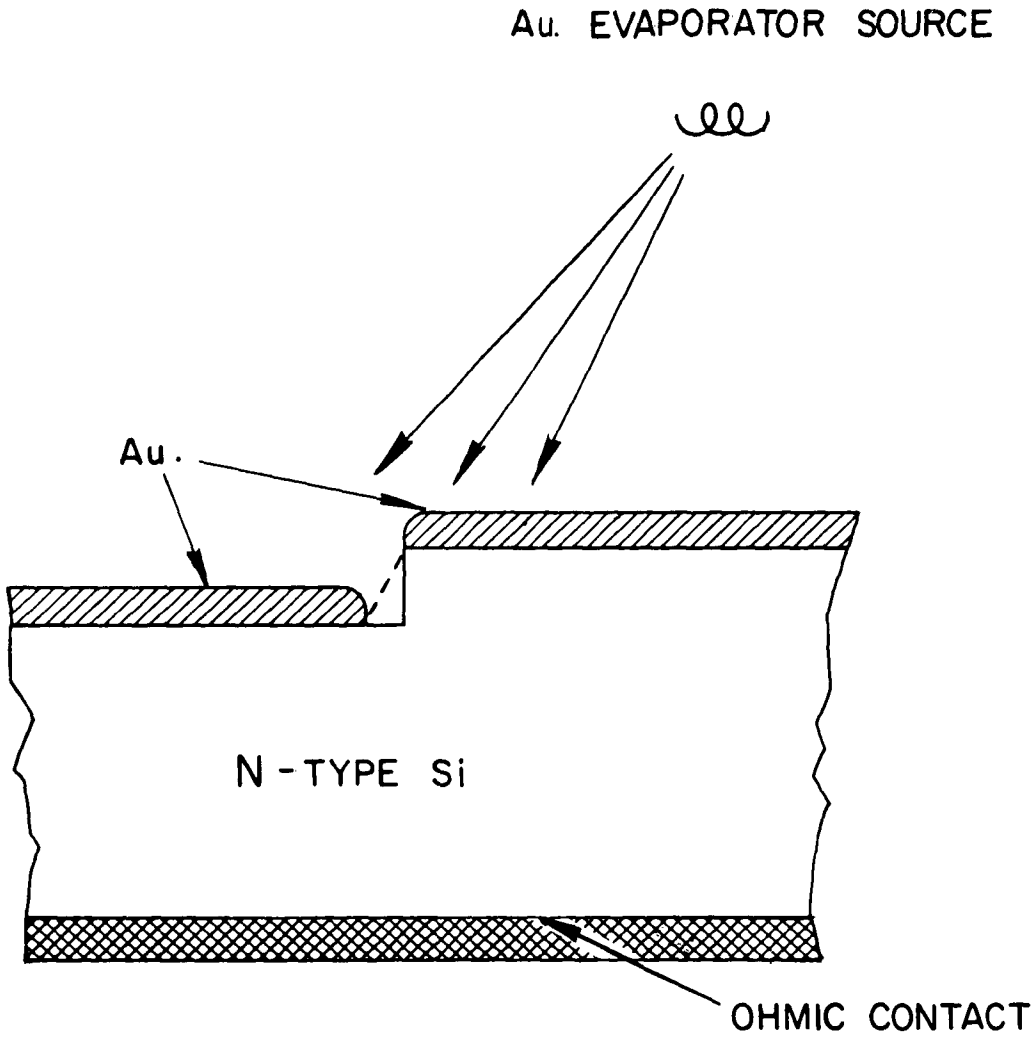

Figure 7. Idealized shadowed deposition of gold on silicon proposed for forming metal edge amplifiers.

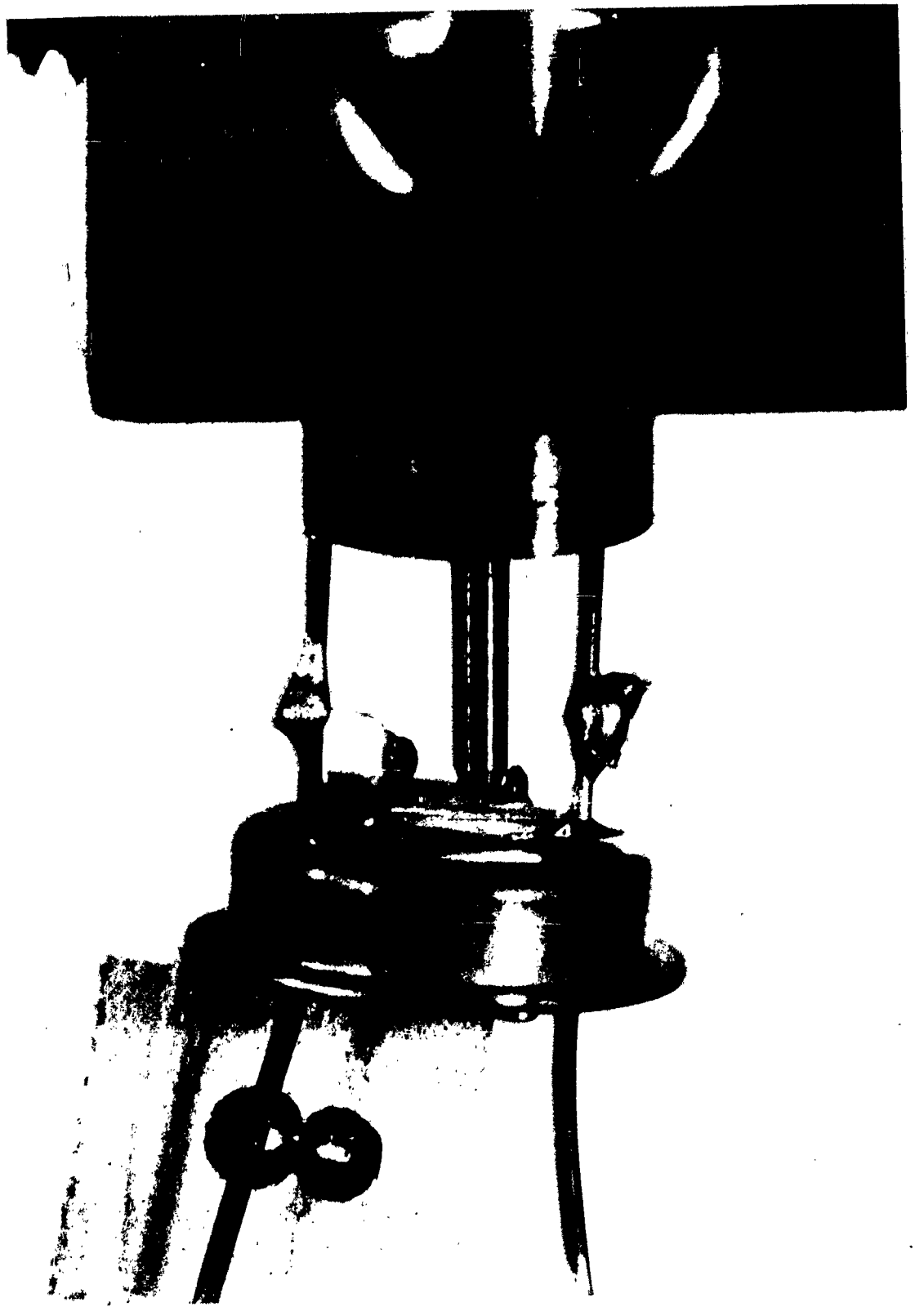

Figure 8. Metal interface amplifier with mercury emitter electrode. 168-63

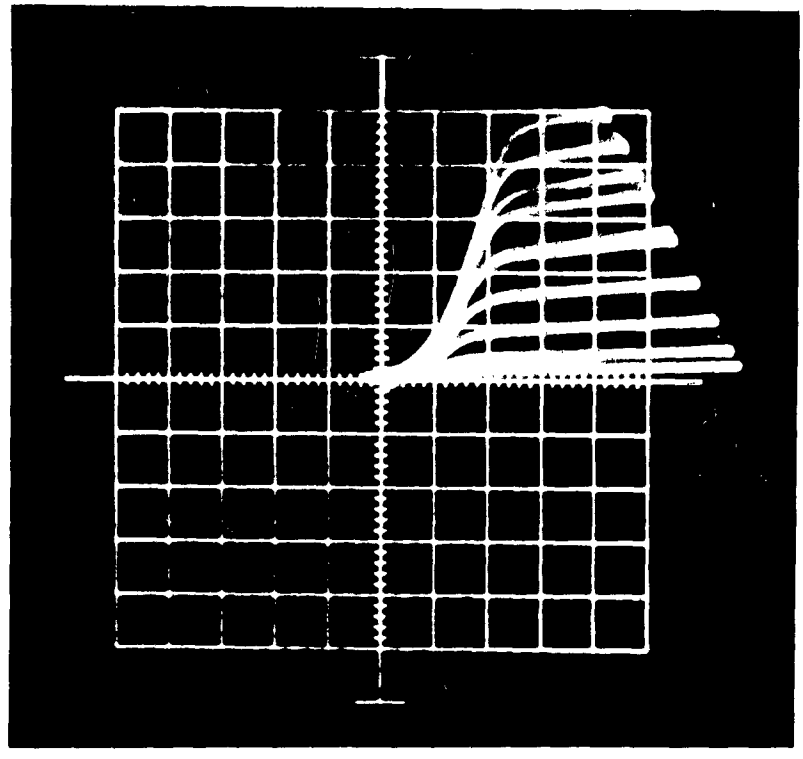

200-63

Figure 9. Collector characteristics of metal interface amplifier with mercury emitter electrode. Vertical collector current scale =0.01 ma. per division. Horizontal collector voltage scale =200 mv. per division. Curve traces at 0.1 ma. emitter current increments.

for such devices is less than 0.1. This typical value for alpha is much less than that observed by Kahng and possibly can be explained by the fact that the surface of the silicon used was exposed to room atmosphere and therefore overcoated with an oxide film. No details have been given by Kahng regarding the preparation of his "suitably cleaned" silicon surfaces but it is suspected that these were cleaved in vacuum. In this event, the oxide films would not have been present.

The operating lifetime of such a device was short, in the range of several minutes, and this observation requires explanation. Some insight into the causes may be obtained by a consideration of the capillary and electrostatic forces that exist within the device. Because the silicon monoxide is very thin, it is very likely that a capillary structure exists within this insulator, even if these capillaries do not represent flaws comparable to pinholes. Because of the high surface energy of mercury compared with that of siliceous materials, the mercury would not wet the capillary when no operating voltage was applied across the emitter structure. However, when the operating voltage was applied, an electrostatic attraction between the mercury (cathode) and the gold (anode) appeared and acted in opposition to the capillary forces. To explain the short life of the device, one need only presume that the electrostatic forces overpowered the capillary forces and that the lifetime of the device was then determined by the viscous resistance to flow inherent in the mercury. The effect of the mercury penetration of the insulating film was to cause the observed alpha to increase from a value less than 0.1 to a value of 1.0. The same change in alpha was also observed when the mercury was placed in contact with a scratch on the surface of the silicon monoxide film. The rise in alpha in these circumstances is to be associated with a deterioration of triode action.

The short operating lifetime of these devices complicated the experiments to some degree, and, as a result, attempts to operate the device as an amplifier were unsuccessful. No voltage or power gain was observed.

No further study of these devices is contemplated at present.

3.3 Diode Structures

Fabrication of diode arrays was continued using procedures described in the previous progress report (ref 7). A modification consisted in overlaying the active areas (where emitter and base layers cross) with a 400-to-600-Å coating of silicon monoxide, by evaporation. This was done for protection against seasonal humidity variations to which these devices are sensitive. At the outset, no shorts such as those encountered during the summer months were observed. However, to check more thoroughly the effects of humidity, saturated salts of the type recommended by the National Bureau of Standards (ref 8) were placed in an environmental chamber to get several standard values of relative humidity for testing devices. The time to obtain equilibrium humidities was monitored by means of a porous graphite-on-silicon contact (ref 9)

developed in the course of some semiconductor surface barrier studies in association with NBS. Adding a small circulating fan reduced this time from several hours to about 20 min. Preliminary results showed little visible change in the I-V characteristics of the diodes as displayed on the 60-cps curve tracer, but further detailed studies of electrical properties as a function of relative humidity and silicon monoxide thickness are required for any conclusive evaluation.

In addition, other aging effects were seen as shown in table I for an array of 12 simultaneously deposited diodes. Initially the units had high resistance and showed only a typical capacitive loop as seen on the low-current (10 μa/div) scale of a 60-cps I-V curve tracer. Two weeks later the resistance decreased to some finite value or zero in some cases, and further decreased with more short-circuits appearing after 6 wk. Crazing of the silicon monoxide layer was observed on some units by this time also. The finite resistance values were determined from the slope of the linear I-V characteristic on the curve tracer in the low voltage range of about 100 mv. This measurement is of special interest when related to tunneling theory in the low-voltage region (ref 3) by the equation (linear with voltage) for the current density.

$$J = \left[\frac{q^2}{h^2 S}\,(2\,m\,\phi)^{1/2}\,\exp\left(-\frac{4\pi S\,(2\,m\,\phi)^{1/2}}{h}\right)\right] V$$

where

q = electronic charge

m = electronic mass

ϕ = internal work function

h = Planck's constant

S = film thickness

V = applied voltage

Various workers (ref 10, 11) have studied this low-voltage region to separate the effects of thickness and barrier height after assumptions concerning the effective mass had been made. This measurement, made with speed and facility, is particularly appropriate to detect aging or other effects where experimental parameters are varied over a range of values. The fall-off of resistance in table I possibly indicates a reduction of the effective insulator thickness by diffusion of metallic ions from the electrodes into the Al_2O_3 spinel structure as proposed by Handy (ref 10), or possible lowering of the barrier height from these same and/or other donor impurities, which tend to convert the oxide insulator to an n-type semiconductor. Further experiments, such as an independent estimate of insulator thickness by measuring its capacitance, are required to determine the cause of this effect.

A method (ref 12) for measuring this capacitance over the wide range of shunt resistances encountered in the above devices was adapted

Table I. Variation of resistance with time of thin-film aluminum-aluminum oxide-aluminum diodes from the same fabrication run.

	RESISTANCE (OHMS)*		
DIODES	INITIAL TEST	AFTER 2 WK	AFTER 6 WK
1	∞	Short	---
2	∞	430	136
3	∞	152	60
4	∞	190	136
5	∞	430	Short
6	∞	680	380
7	∞	440	128
8	∞	220	80
9	∞	250	Short
10	∞	400	20
11	∞	184	Short
12	∞	1900	Short

*The resistance given here is a low-voltage value, viz: $\Delta V/\Delta I$ for $\Delta V \sim 100$ mv. The resistance is designated as infinite when only a capacitative loop is observed on the oscilloscope (cf text).

and refined. This technique is particularly suited for measuring any high dissipation or low Q impedance where most bridges fail. The circuit, shown in figure 10, is essentially an attenuator network of standard and unknown impedances in series, where the output voltage observed across the unknown is compared in amplitude and phase with the input. A null occurs when impedances are adjusted so that an ellipse degenerates into a straight line of slope equal to one-half on an oscilloscope display. For the pure resistance and capacitance of immediate concern, this occurs when $RC = R_oC_o$, independent of frequency. Here R and R_o and C and C_o are the resistances and capacitances of the unknown and standard impedances, respectively. Fortunately, this frequency independence yields a dividend in that an extra fine null is obtained by varying the frequency simultaneously with the standard capacitor, until no ellipse is seen when the frequency alone is varied (impossible on a fixed-frequency bridge). The use of an external attenuator and amplifier, in turn, permits the calibration of slope one-half when $R = R_o$ and $C = C_o$. Also, the a-c signal can thereby be reduced so that small signal impedance values may be determined for highly nonlinear devices. In this way a 17-mv signal was applied to the diode itself. D-C biasing was attempted through an rf choke, but its distributed capacity prevented getting the required null. Further work is required to develop bias from a high-impedance source such as a pentode. Measurements made at zero bias on diodes of table I gave values of conductance and capacitance in substantial agreement with those made by substitution methods using standard decade boxes. An average capacitance value of 1.52 $\mu fd/cm^2$ with a maximum variation of 0.12 $\mu fd/cm^2$ was found indicating a relative uniformity of thickness and dielectric constant for units of various areas on a microscope slide. Thus it appears that diodes under study may be characterized by a thickness in units of capacitance per unit area, following Mead (ref 12) which can be compared with direct thickness measurements on a control slide obtained from the same evaporation run, when diode arrays are fabricated.

3.4 Film Thickness Measurements

In the previous progress report (ref 14), a description was given of a prototype multiple-beam interferometer that had been built to measure the thickness of films making up the tunneling structures. Although this equipment was already an improvement over the slightly modified metallurgical microscope used even earlier, experiments with the former indicated a number of shortcomings and ways to overcome them. Accordingly the multiple-beam interferometer was completely rebuilt and in its present form is shown in figure 11. A comparison with figure 12 of the previous report makes many of the improvements obvious. The second model is equipped with a camera that includes a coupled visual system for securing a more critical focus through the eyepiece than is possible through the ground glass. The camera support has been made integral with the working platform supporting the stage interferometer, and it has been designed for maximum rigidity. In addition to the coarse and fine rack and pinion for positioning the working platform, a two-jaw vise, with nylon jaws, is provided to clamp the platform rigidly in place when optimum focus has

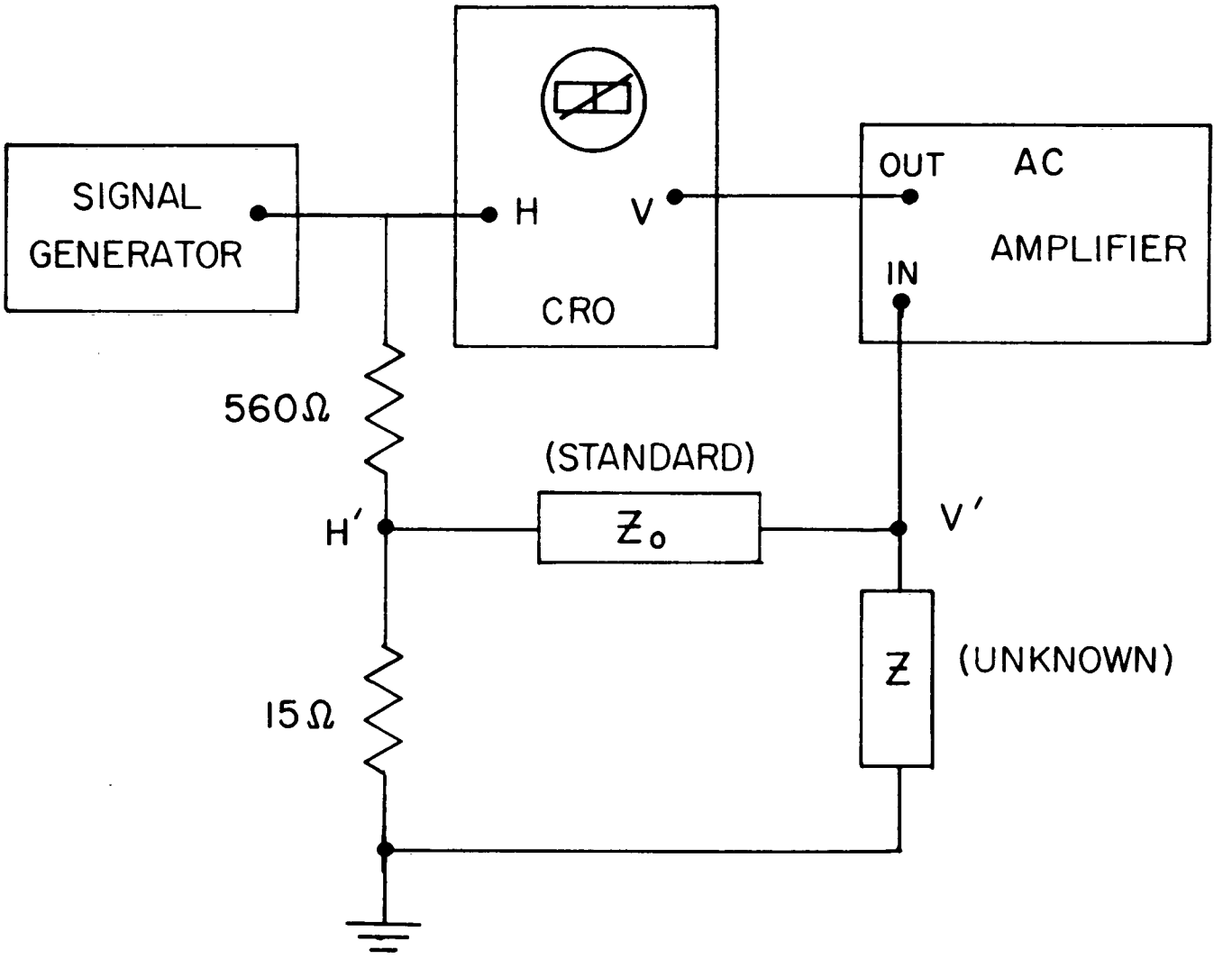

Figure 10. A small signal, low-Q impedance measuring circuit. Z_o (standard impedance)=R,C and/or L decade boxes. Z (unknown impedance)=Diode or triode imput, etc. When $Z=Z_o$, ellipse collapses to line of slope 1/2 on CRO.

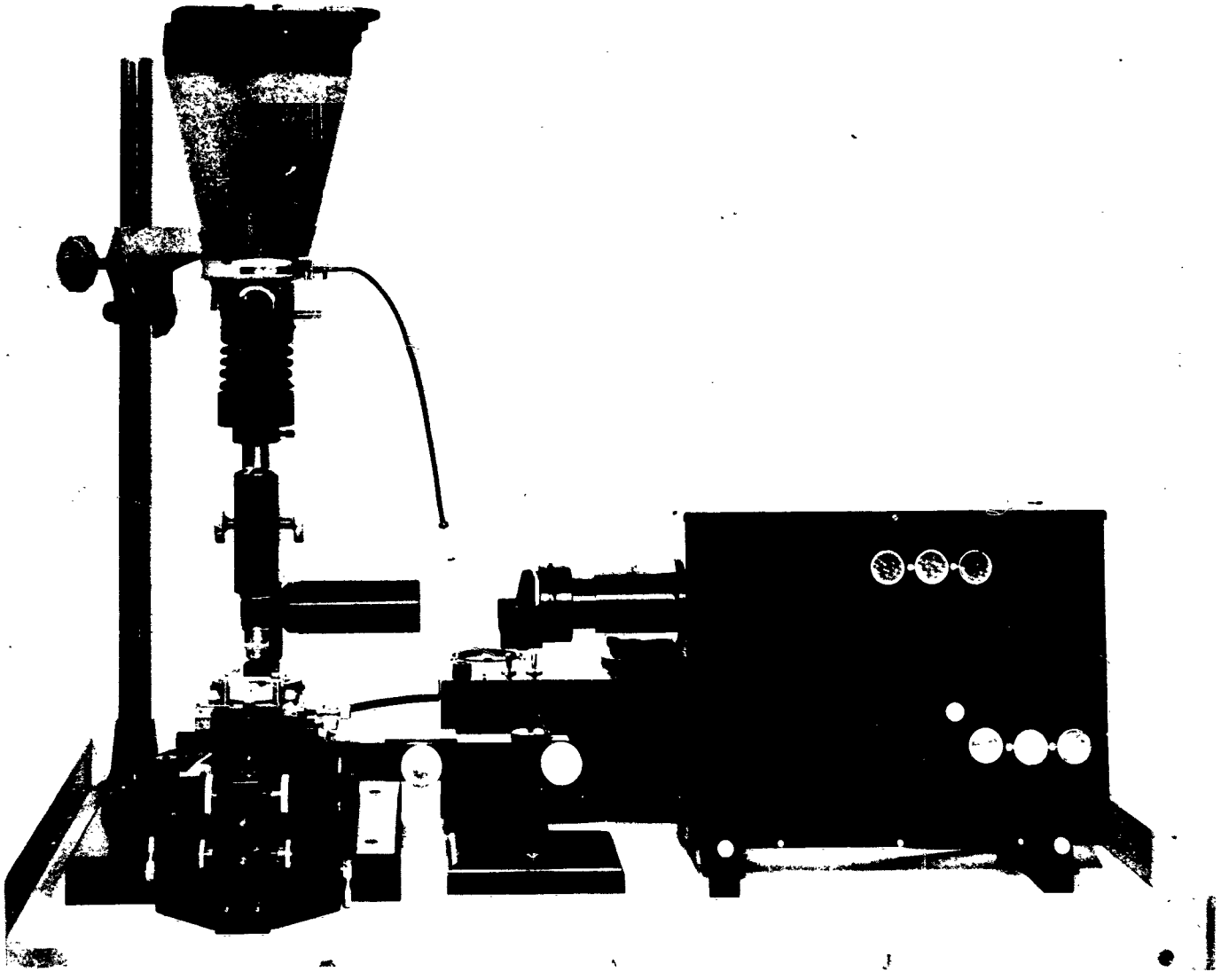

Figure 11. Multiple beam interferometer assembled during the period reported. 169-63

been obtained. The new stage interferometer is similar in principle to that used in the prototype but has been designed to hold a 2-in. diameter optical flat rather than a microscope slide above the specimen. Flexure springs secure the flat and the specimen slide in a vibration-free manner and hardened steel ball points at the unclamped end of the stage interferometer prevent this subassembly from vibrating relative to the working platform. Except for the addition of a flexible light trap at the eyepiece end of the microscope body tube, the arrangement of the latter and the vertical illuminator is substantially the same as before. The collecting lens in the microscope illuminator is now a high-quality achromatic doublet that has been antireflection coated.

Only minor mechanical changes have been made in the lamphouse. The lens tube and filter holder have been redesigned to accommodate an achromatic doublet, in place of the singlet lens formerly used, and to secure the interference filters exactly normal to the axis of the beam in a vise-like clamp. This feature eliminates off-axis beams arising from multiple reflections from the filter faces. These are especially annoying when several filters are used in series, as, for example, when neutral density filters are inserted after the spectral line filter for viewing the interference pattern visually through the microscope eyepiece. The light source presently in use is the Osram mercury spectral lamp, which represents a very good compromise between reasonably high light intensity and very low pressure broadening of the spectral line. This lamp is operated on a 220-v power line in series with a variable ballast resistor and ammeter. The use of a resistive ballast rather than a reactive ballast recommends itself in this application because the former represents a hum-free system. The ballast resistor and the lamp are each cooled by a gentle stream of air provided by a small blower not shown in figure 11. The blower is secured to a wall-mounted shelf so that its vibration is not transmitted to the base plate of the instrument; flexible ducts direct the air streams to the appropriate points.

A new feature, which is partially visible in figure 11, has been added to the interferometer. This is a train of three pentaprisms that can divert the parallel beam from the lamphouse, down, across, and up through the bottom of the stage interferometer, so that the interference pattern can be formed in transmission instead of in reflection. The vertical member containing the first pentaprism to encounter the light beam is removed when the interferometer is used in reflection, as is the case in the figure. All the subassemblies are bolted down to a flat metal base plate as before, but in the present arrangement the plate has been covered with linoleum to provide a better working surface; and a wooden edging has been added. The plate is isolated from a table below by rubber shock mounts.

The changes enumerated above and improvements in experimental technique are reflected in a considerable improvement in the fringe systems obtained. In figure 12 is shown a set of Fizeau fringes taken with the interferometer as it has just been described; these may be compared with the earlier fringes in figure 11 of the previous progress report. The

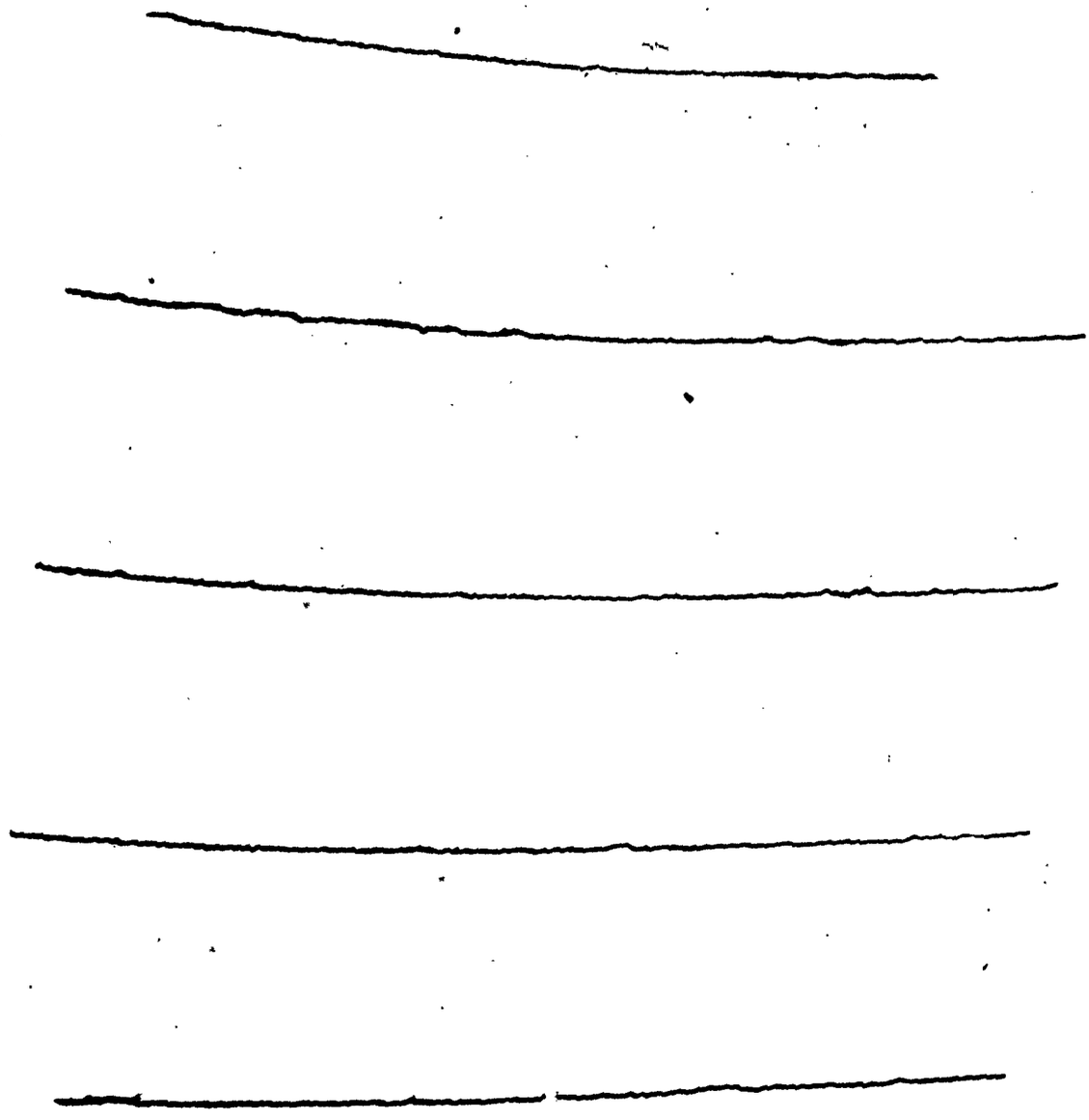

Figure 12. Fizeau fringes formed between an optical flat and a microscope slide.

improvement is marked. The fringes of figure 12 were formed between an optical flat that had as its reflecting surface a 7-layer dielectric coating and a microscope slide with a 9-layer dielectric coating. Both coatings were designed (by an outside company) to have maximum reflectance at the 5461 Å line of the mercury spectrum, which was used in these experiments. Because the mechanical and optical revision of the apparatus required most of the report period to complete, there has been little time to make a detailed study of the optical performance of the apparatus. However, some vital statistics of the fringe system shown, taken hurriedly and accordingly to be considered approximate, will serve to indicate the performance to be anticipated. The fringes were formed on a 4 by 5 in. Eastman metallographic plate at an optical magnification of 20 diameters. The plate was exposed for 10 sec and developed 6 min in Kodak D-60 developer. A contact print was made and inspected by means of a measuring microscope. The ratio of the fringe width to the distance between fringes was less than 1:100. The wiggles in the fringes are due to irregularities in the reflecting surface of the optical flat and probably have their origin in polish marks. They are not observed when the optical wedge is formed between two coated, fire-polished microscope slides. The wiggles correspond to hills and valleys in the surface of the flat, and two adjacent valleys near the center of the illustration were measured to be 43 Å and 38 Å. The 5-Å difference between them seemed well established. The plate was enlarged 1.5 times to make the figure so that the optical magnification shown here is only about 30 diameters. Even so, the magnification of the profile provided by the fringe system is about 150,000 times. It is apparent that the original requirement, viz: to be able to measure a 25-Å step to within a certainty of 5 Å is within the reach of the instrument as it now stands. It must be recognized that it is not possible to measure a 25-Å step if the matching surface has ripples in it of the same magnitude. For this reason, several microscope slides have been given reflecting coatings to HDL specifications and, although they are not optically flat, their surfaces are presumably ripple-free. There has not yet been time to exploit these.

Relatively little further mechanical work remains to be done on the interferometer, as such. The present arrangement of flexure springs and screw-adjusted lifting levers for adjusting the strike and dip of the matching surface leaves much to be desired. A new stage is under construction in which the flexure springs and lifting levers will (hopefully) be unnecessary and the screw adjustments will be replaced by differential screws designed for 0.003-in. travel per turn. Further work in this connection will be directed mainly toward perfecting the technique of measuring small film thicknesses.

The interferometric method depends upon measuring the shift of the Fizeau fringes as they pass over the edge of the film to the substrate below. With base metals, the oxide layer grows rapidly over all the exposed surface, and it follows that it is impossible to obtain a step corresponding to the thickness of the normal oxide layer. Such oxide films cannot be measured accurately by the interferometric method, and, in particular, the thickness of the oxide layer on aluminum cannot be

accurately measured in this way. Gold is the only metal that remains oxide free, and insulating layers on gold can be accurately measured interferometrically. Likewise insulating layers deposited over oxidized metal surfaces can be so measured as can the thickness of metal plus oxide layers. To measure the thickness of naturally occurring oxide layers, one must use the ellipsometer. This instrument senses the change in properties of polarized light, after reflection from the oxide-covered surface. The theory underlying this instrument is recondite (ref 15, 16). In the practice of this measurement, a parallel, monochromatic beam of light is reflected obliquely from the surface under examination. The incident beam is elliptically polarized so that the reflected beam is plane polarized. From the azimuth and ellipticity of the incident beam, and from the azimuth of the reflected plane-polarized beam, the thickness and the refractive index of the oxide layer can be determined in principle. In reality, the optical constants of the oxide-free metal must be known, and these, in general, cannot be measured with the ellipsometer alone. Furthermore, the computation is of such magnitude that it can be done practically only on a digital computer. Where applicable, the method is extremely sensitive and is capable of determining films less than 10 Å thick.

Because of the power of the method, it was of immediate interest for this program. A purchase order for a photoelectric ellipsometer was initiated during the preceding period, since it appeared that the photoelectric instrument would be more useful than the purely optical type. In retrospect, this may have been a poor decision because the former are supplied by a single manufacturer and deliveries are unusually slow. Delivery to HDL is not expected before March 1963. In the interim, a detailed study of the theory of this measurement has been made, and an arrangement has been made with a group at the National Bureau of Standards whereby small amounts of time may be borrowed on their ellipsometer. While this is not a convenient arrangement, it is a considerable help nevertheless. They have also made available a computer program that HDL has recoded for the HDL-IBM 1410 computer. The principal problem remaining in the use of the ellipsometer resides in the requirement for the optical constants of the unoxidized base metal. The only practical way to determine these is to construct a special vacuum system in which the ellipsometry can be done upon the metal film both before and after oxidation. Such a system is necessarily complicated, but a design that approaches this problem in as simple a way as possible is being developed. In the meantime, attempts will be made to use values of the optical constants published in the literature. Because optical constants for metals are dependent upon the manner in which the metallic films are prepared, an unknown uncertainty is introduced by the use of literature data. The experiments with the ellipsometer are just now beginning and as yet there are no results to report.

3.5 Thin-Film Semiconductor Experiments

During this period, work has continued on the deposition of cadmium sulphide films. Early attempts to evaporate CdS powder from

resistance-heated open boats were not very successful; rates of evaporation were low, often being below the rate required for film formation on glass. Use of the electron beam evaporator enabled higher evaporation rates to be reached, and good adhesion to glass substrates was obtained. A satisfactory evaporation rate is about 100 Å/sec (with a target distance of 40 cm) and is obtained with a beam power of 150 w. The highest evaporation rate attempted was approximately 450 Å/sec giving a film thickness of 5μ (for a 2-min evaporation) with good adhesion to a glass substrate.

Preparation of the bulk material and the choice of crucible are practical considerations to be taken into account. Loose CdS powder in a crucible is unsatisfactory because it gets ejected around the chamber. To avoid this, cylindrical pellets of CdS were formed by hydrostatically pressing CdS powder with pressures of 10,000 lb/in.^{2} over the surface of the pellet. Evaporation from a compacted pellet is satisfactory, but, since the pellet may crack, it must be contained in a crucible. Crucibles formed from insulating ceramics build up electrostatic charges that repel the electron beam, thus preventing the CdS from being heated. To overcome this problem, crucibles were made from carbon with an outer shell of stainless steel as shown in figure 13. Small vertical grooves were made on the outer surface of the carbon crucible to allow for gas evolution during heating. The crucibles have been used with a wide range of materials, the carbon "liner" providing a good compromise for the conflicting requirements of a crucible with good electrical conductivity and low thermal conductivity.

The second half of the period saw the completion of the simple mask changer for the electron-beam evaporator. The mask changer shown in figure 14 is manually operated from outside the chamber and has five stations. The substrate holder has provision for two 3-in. by 1-in. substrates plus three substrates for thickness measurements. Thus in one pump-down of the chamber, five depositions can be made, of which three can be monitored. It is therefore very convenient for use in the fabrication of multilayer structures. No provision is made for heating the substrates, but such a facility could be added if required.

CdS films deposited onto glass substrates at room temperature have a metallic appearance. It is thought that this is due to free Cd in the film, because on heating the film (under vacuum of 10^{-5} Torr) at 350°C for approximately 1 hr, the film reverts to the normal orange color of CdS. It is considered that the free Cd diffused through the film and is evaporated (mp of Cd is 320°C). The electrical resistivity was found to have increased by two orders of magnitude after the heat treatment.

Using the mask-changer and a set of masks, primarily designed for capacitor investigation, a number of multilayer structures were made. Structure systems fabricated included In-CdS-Ge-Au, Al-CdS-Ge-Au, and Al-CdS-Au. The first two were attempts to detect rectifying properties between CdS n-type layer and Ge layer, which previous experience (ref 17) had indicated would be p-type. These four-layer structures were short-circuited between the outer layers, but, using an Au probe on the uncovered

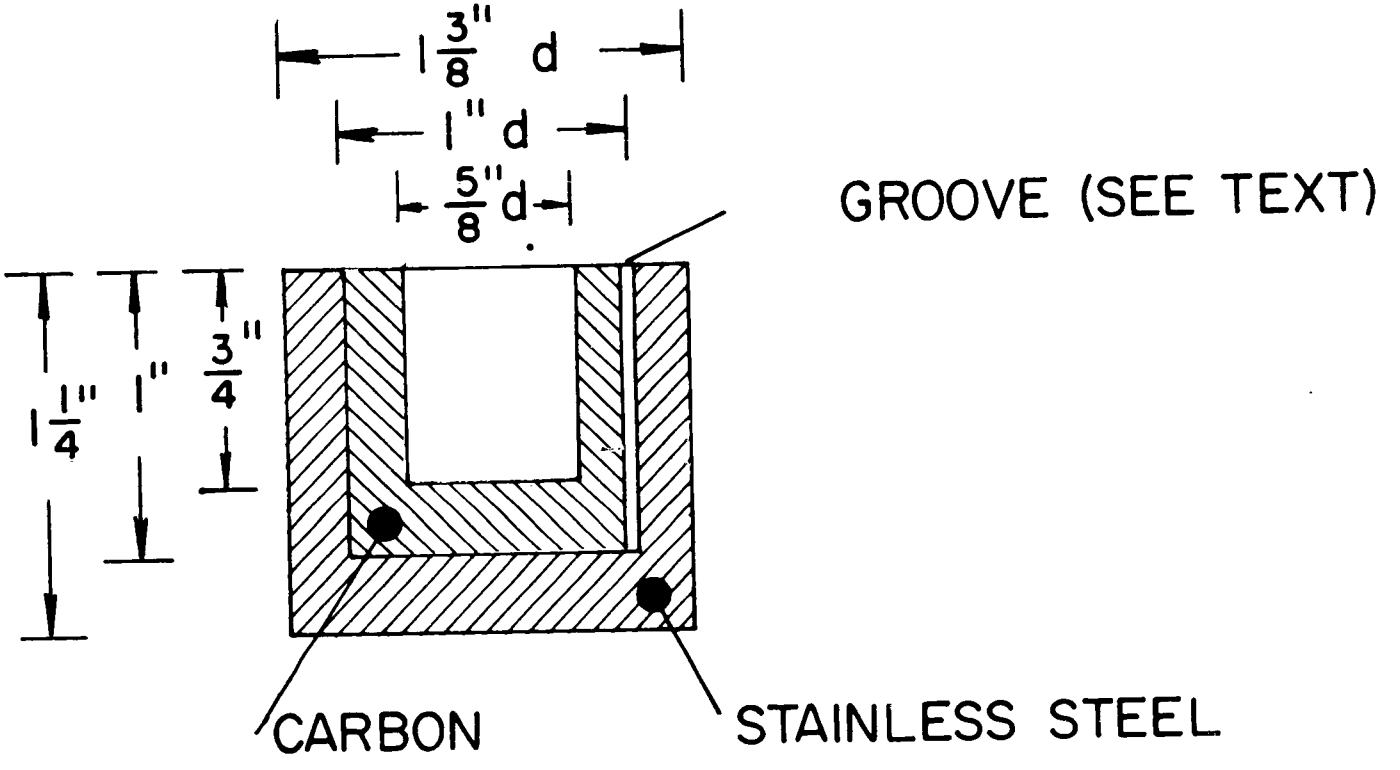

Figure 13. Crucible for use with electron beam evaporator.

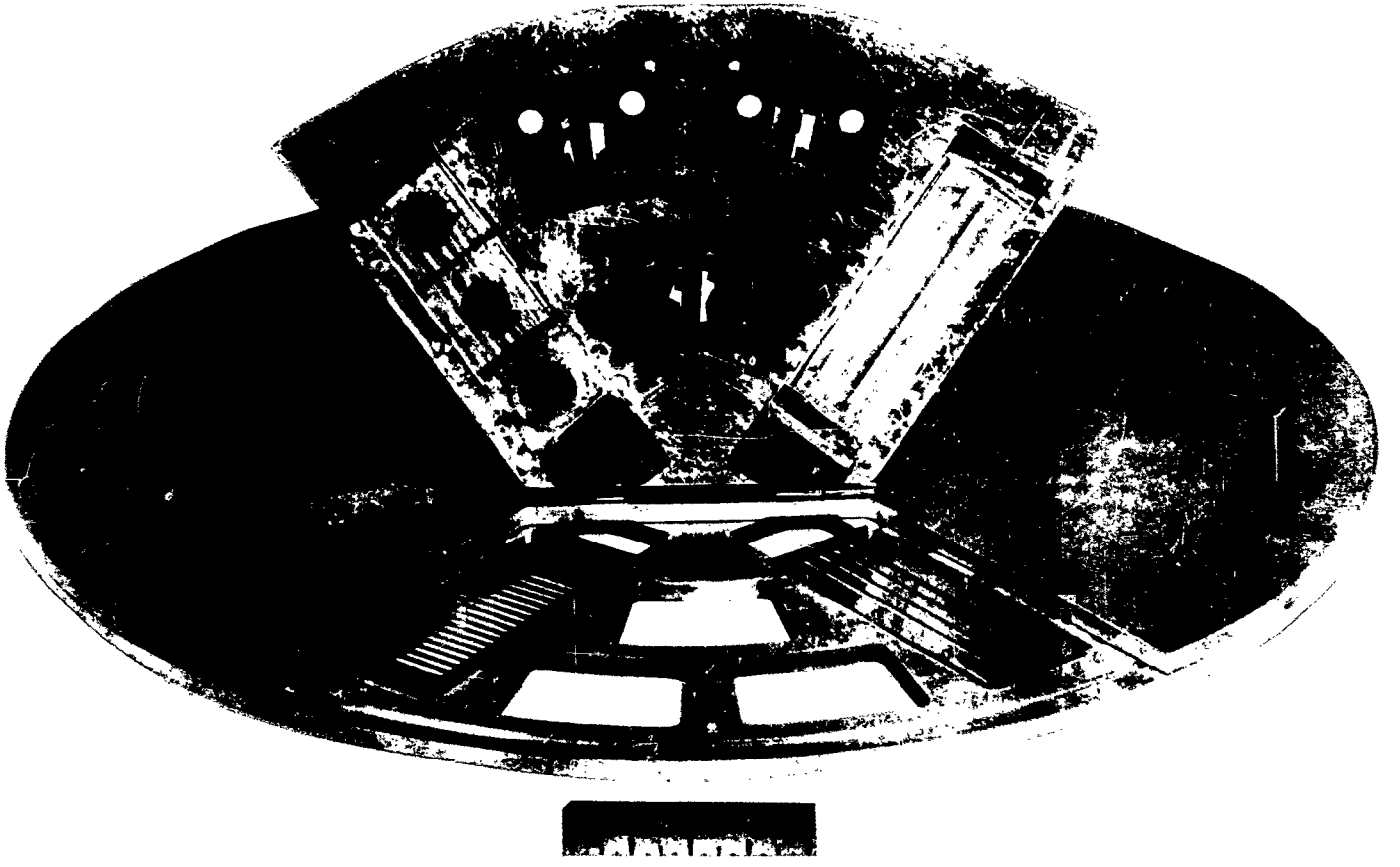

Figure 14. Mask changer for use with electron beam evaporator. 209-63

part of the CdS layer, small areas were found that gave a rectifying characteristic, while other areas were short-circuited. This led to the fabrication of the three-layer system, Al-CdS-Au. Again short-circuits occurred between the outer conducting layers. Since the areas were large ($\approx$ 1 cm^2), further systems were fabricated in which the third layer was replaced by a number of independent areas ($\approx$ 1 mm^2). In this case when contact was made to these small areas, some showed rectifying properties while others were short-circuited. It was difficult to make contact to these films without damaging them, and the short circuits were thought to be caused by damage to the films rather than faults within the film.

With the experience of these experiments in mind, a new set of masks was designed and are nearing completion. With these masks it will be possible to deposit 76 three-layer structures on a 3 in. by 1 in. glass slide and by means of the extended conductors, the structures will be tested individually (fig. 15). Furthermore, damage due to probe pressure of the structures that are of interest will be avoided.

4. PROGRESS—ADMINISTRATIVE

4.1 Historical Survey

In the previous progress report the background and history of the thin-film, hot-electron triode were reviewed (ref 18). This survey is continued here and its scope has been broadened to include other thin-film active devices that need not be hot-electron devices but are still likely to be radiation resistant as related to this contract. Specifically, two thin-film triodes based upon a space-charge-limited current mechanism and not previously treated in these reports will be described.

The feasibility of a solid-state electronic device based upon the modulation of a space-charge-limited current was first demonstrated by Ruppel and Smith of RCA (Zurich) (ref 19), who used single crystal platelets of cadmium sulfide for the semiconducting material. The theory underlying space-charge-limited currents in solids predicts the conduction of large currents through wide bandgap semiconductor (i.e. insulator) films, provided electrons can be injected into the conduction band and that their mobility there is reasonably high, and provided also that the concentration of structural defects that give rise to electron-trapping states for the otherwise mobile electrons is low. Space-charge-limited conduction is characterized (under a particular set of conditions to be described below in connection with the construction of actual devices) by a current depending upon the square of the applied voltage and the inverse cube of the separation between the electrodes. Such success in relation to these devices as is being achieved presently owes much to the broad study of conduction phenomena pursued for many years by Rose and his colleagues at RCA Laboratories (Princeton)(ref 20, 21). It was these studies that indicated the desirable properties of cadmium sulfide in this connection. An analysis of space-charge-limited currents in cadmium sulfide as applied to solid-state device design has been given by Wright (ref 22).

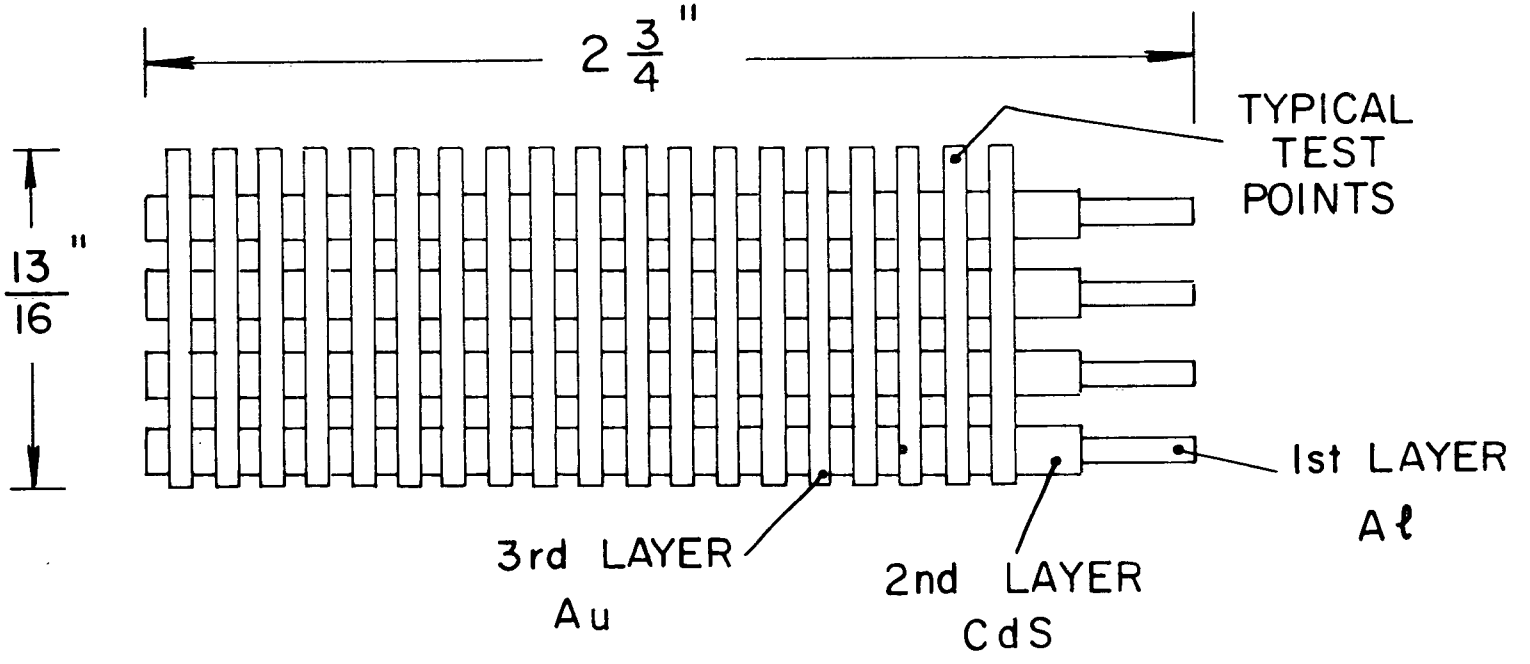

Figure 15. Crossed-over pattern to be fabricated with new masks.

The construction of thin-film devices employing space-charge-limited currents proceeds along the following lines: a diode or rectifier results when one metallic contact to the cadmium sulfide is ohmic (i.e. presents no barrier to thermal electrons injected from the metal electrode into the conduction band of the insulator) and the other contact is a rectifying contact (i.e. presents a high barrier to the thermal electrons)(ref 19). If the former is made the cathode and the latter the anode, the diode will be forward biased and space-charge-limited current will flow. If a third contact is appropriately interposed between the cathode and anode, the possibility of modulating the current to obtain triode action arises. If this third electrode is insulated from the cadmium sulfide by a suitable nonconducting film, either positive or negative bias may be applied to it to increase or decrease the load current, without drawing appreciable current through this electrode. Such a device will be capable of power gain. It is now apparent that it is not absolutely necessary to have a rectifying contact in the original diode, although this may be desirable in some cases. Likewise if the third electrode were a rectifying contact and hence isolated by its own potential energy barrier, only reverse bias relative to the cadmium sulfide could be applied for successful device operation.

The triode takes two similar geometrical forms with their associated modes of operation. These are illustrated in figure 16, which shows the cadmium sulfide film on an insulating substrate with several metallic electrodes attached. In order to realize appreciable space-charge-limited currents, the dimensions of the device must be small--generally of the order of tens of microns. The smallness of these dimensions introduces difficulties in fabrication that have nevertheless been surmounted by Weimer of RCA (Princeton) (ref 23), who has developed the first truly thin-film active device along the lines discussed here. Terminology relating to field effect transistors has been used to describe these devices because of obvious similarities, and thus the electrodes are appropriately called the source, gate and drain as shown in the figure. Tantraporn of General Electric (Syracuse) describes these devices in a recent review (ref 24).

Weimer's "field-effect" configuration can be represented in figure 16 by using only the upper source in connection with the gate and drain. The gate can be biased negatively to deplete the electrons from that portion of the channel between the source and drain, which is adjacent to the gate electrode. Increasing the negative bias increases the width of the channel that is depleted. This variation of effective channel cross section as a function of gate bias voltage modulates the current as in the unipolar transistor (ref 25). It should be noted, however, that here the mobile electrons injected into the space charge are controlled rather than the equilibrium electron density in the semiconductor, as in a conventional unipolar device (ref 23). By virtue of the insulated gate, Weimer's (gate) triode can be (forward) biased to increase the electron density in the channel. In fact, this "enhancement" or "enrichment" mode yields much higher transconductance (>10,000 μmhos) than the depletion mode. Furthermore, the output current-voltage characteristics resemble

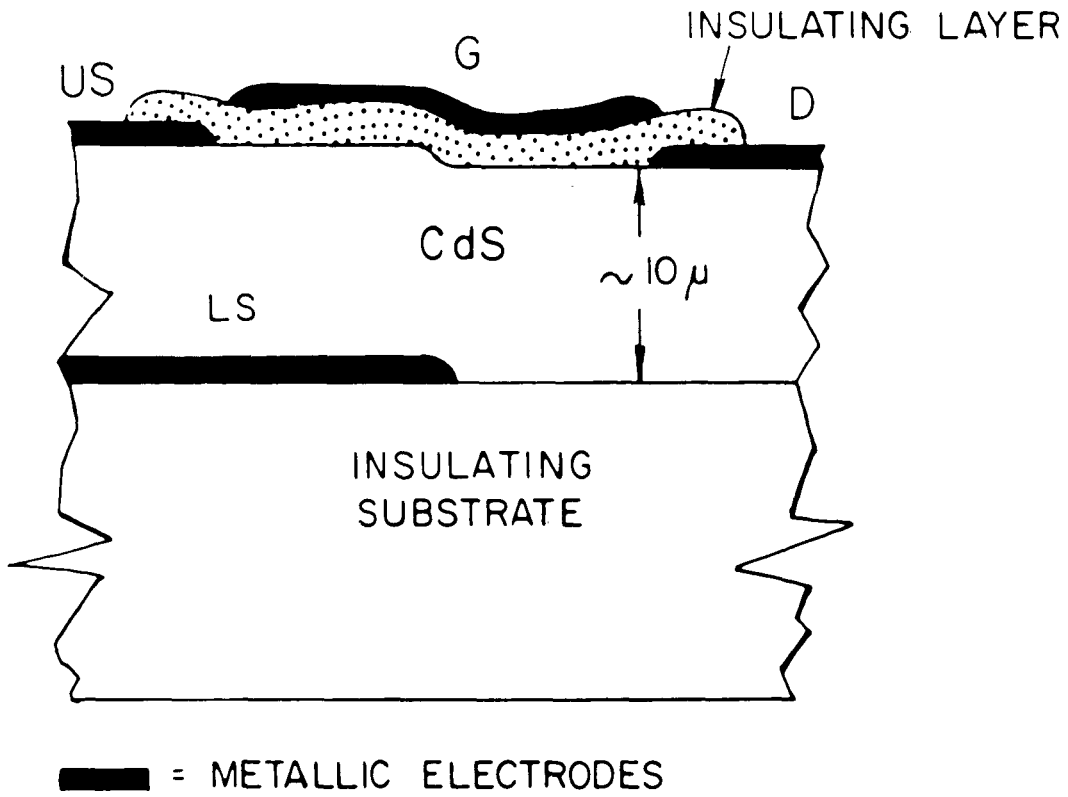

Figure 16. Thin film space-charge-limited triode geometry.

Analog type: when the lower source (LS) is used in conjunction with the gate (G) and the drain (D) resulting in vacuum triode-like I-V characteristics. Field-effect type: when the upper source (US) used with the gate (G) and the drain (D) resulting in pentode-like, saturating characteristics.

those of the unipolar, or field effect, transistor in that they saturate at constant bias not unlike those of the pentode vacuum tube. This is explained by Weimer as being due to the remoteness of the drain from the source, which makes the drain potential substantially unable to penetrate to the source. A similar situation exists in the conventional unipolar transistor. Thus the gate controls the conduction process beyond some threshold drain voltage, just as does the control grid, shielded from the plate by the screen grid in a pentode tube.

The "analog" triode configuration is also depicted in figure 16, if the device is operated by using the lower source in conjunction with the gate and drain. In this case, the lower source electrode extends over into the gate region, as in the original design of Ruppel and Smith (ref 19). This circumstance permits the field from the drain to penetrate into the source and gate region at all voltages. This results in operating characteristics resembling those of a vacuum triode. An obvious extension to multiline or mesh grids for higher transconductance by masking techniques is possible, as pointed out by Weimer (ref 23). This same goal could be obtained by various combinations of upper and lower electrodes, resulting in hybrid field effect-analog structures, as treated by Tantraporn (ref 24).

A comparison of the two configurations in working devices (ref 19, 23) shows both having high power gain ($\simeq 10^5$) because of the high input impedance ($> 10^8$ Ω) of the gate electrode. Thus far, however, the field-effect type has a high transconductance (> 10,000 μmhos) while that of the analog type is very low (~ 10 μmhos). Similarly, the output impedance of the field-effect type is high (> 1 meg) compared with that of the analog type (~ 100 K). This results in a higher voltage gain (> 100) for the field-effect type compared with that of the analog type (< 1). The high transconductance of the field-effect device also yields the large figure-of-merit ($G_m/C > 10$ Mc) reported by Weimer.

According to the analysis of van der Ziel, which appeared during this report period (ref 26), this class of devices promises lower noise than do diffusion-type devices such as the transistor, because of the space-charge mechanism. The trapping mentioned earlier, which limits the d-c transconductance, will disappear at high frequencies (i.e. beyond the reciprocal relaxation time for the traps) so as to enhance the high-frequency response of these devices, according to Wright's analysis (ref 22). The well known photoconductive properties of CdS suggest an extension to phototransistor applications (ref 20, 21). Weimer reports an output current and thus transconductance increase of about four times in going from the dark to 20 fc of light (ref 23). In the same paper he also describes the fabrication of integrated thin-film circuits with these triodes, e.g., a three-stage direct-coupled amplifier, and logic circuits such as flip-flops, AND and NOR gates.

A final comment might be made that these devices, based on majority carrier transport, would be resistant to the type of radiation that deteriorates minority carrier lifetime, but not to that which introduces appreciable trapping defects. The latter could be good or bad, depending upon whether the high-frequency response is improved (as noted above), or the space-charge injected current is substantially reduced. This would

probably require radiation levels in these polycrystalline films far above those that damage transistors.

In general, no outstanding breakthroughs in thin-film or radiation-resistant devices were noted during this period. Rather, refinements of device structure and consolidation or critiques of theory and experiment are in evidence. Several technical meetings deserve some attention here.

The National Electronic Conference (NEC) at Chicago, Illinois, 8-10 October, sponsored a paper by W. Tantraporn and K. Reinhartz (ref 24) on field-effect triodes, covered in the above discussion of space charge limited (SCL) devices. Other thin film devices were also reviewed as to state-of-the-art and expected performance.

At the Electron Device Meeting (EDM) sponsored by the Professional Group on Electron Devices (PGED) of the IRE at Washington, D. C., 25-27 October, J. Moll of Stanford compared hot electron and related active devices in detail. He concluded that the transistor has the highest theoretical alpha-cutoff frequency, f_{co}, followed by the metal base transistor (MBT) discussed in a previous report (ref 27) with ~ 67 percent f_{co}, the SCL triode with ~ 33 percent f_{co}, and the Mead tunnel emission amplifier (TEA) with ~ 1.5 percent f_{co}. However, the maximum frequency of oscillation, f_{max}, of the transistor fared differently, the MBT ranking highest with ~ 10 f_{max}, the SCL triode with ~ 5 f_{max}, and the TEA with $\sim f_{max}$. Note that all rank with or above the transistor as oscillators. These comparisons must be viewed with caution, however, as not all-inclusive or anticipating breakthroughs such as the Philco metal-edge amplifier (MEA) or modified MIA pointed out in the device comparison of the previous report (ref 28).

At this same meeting, R. Schwarz and colleagues from Philco further discussed theory and measurements on MEA devices, reporting oscillations at 42 Mc, and power gains of 10 db at 10 Mc.

The Northeast Research and Engineering Meeting (NEREM) held at Boston, Mass., 5-7 November, posted two papers of interest. H. Borkan and P. Weimer gave a paper on the SCL triode discussed above (ref 23). M. Atalla of Hewlett Packard Associates reported developments on the MBT with Si-Au emitter giving injection efficiencies of about 0.998.

Finally, the 9th National Vacuum Symposium of the American Vacuum Society at Los Angeles, California, 31 October - 2 November, sponsored a host of papers on supporting technology for thin-film devices that can only be briefly summarized here as covering the preparation, growth, structure, and properties of thin films, and associated technology, such as, evaporators, diffusion and getter-ion pumps, vacuum gauges, leak detectors and mass spectrometers. A paper was also presented by D. McNeill and D. Contini of Martin-Orlando about research on tunnel emission in sandwiches and Mead triodes.

The status of thin-film devices as of December 1962, can be summarized by Tantraporn's review (again not all-inclusive) mentioned above, which appropriately appears in the December issue of Electronics (ref 24). The SCL triodes are characterized as voltage controlled through a high input impedance with low noise and high gain-bandwidth product (10^8 - 10^9 cps), whereas the hot carrier triodes are current controlled through low input impedance with higher noise and a lower gain-bandwidth product (10^6 - 10^7 cps) limited by input capacitance. Note the disparity of this analysis with that of Moll's above, which rates the MBT, a hot carrier device, with the highest frequency performance. Achievement dates for these devices in thin film form are listed as 1961 for the field effect version of the SCL triode, 1963 for the analog version, and late 1963 for the hot carrier triode.

4.2 Contract Effort

Work has proceeded on both contracted programs as reported in the monthly letter reports prepared by HDL for NASA. The Philco Corporation has emphasized experimental techniques, the theory of collector efficiency and the fabrication of thin-film triodes called metal-edge amplifiers. The General Electric Company has concentrated upon the fabrication of tunnel-emission cathodes utilizing ultra-high-vacuum techniques. Both organizations have issued their first quarterly progress reports, and these will receive the same distribution in NASA and HDL as the present report. Since the contract work was coordinated by the Department of Defense, Advisory Group on Electron Devices (AGED), which has the policy of wide dissemination of the results of government-supported work, both contractors will distribute copies of their quarterlies to specialists throughout the industry.

5. PLANS

Table II illustrates the overall program in radiation-resistant devices as supported by NASA. Included on the right is the Signal Corps program at Philco, which was coordinated with the NASA-HDL effort through AGED.

In HDL the experimental work will be concerned with two major programs. These are (1) the use of cadmium sulfide as a collector of hot electrons and (2) the dependence of the I-E characteristics of tunnel emitters on insulator thickness and temperature. The insulator thickness will be measured optically. In the collector work it is hoped that techniques will be improved to the point where intrinsic cadmium sulfide can be used as an insulator in a Mead-type collector or, when suitably doped, as an n-type semiconductor in a Spratt-type collector.

In the past, HDL has attempted to duplicate published work on thin-film triodes. Triode action has been observed in devices of Mead, Spratt, Lavine and Kahng types but no valid determination of power gain has been possible. The present plans include a major decision to defer triode work at HDL and to concentrate on tunnel emitter experiments.

TABLE II. NASA - HDL PROGRAM IN RADIATION RESISTANT DEVICES

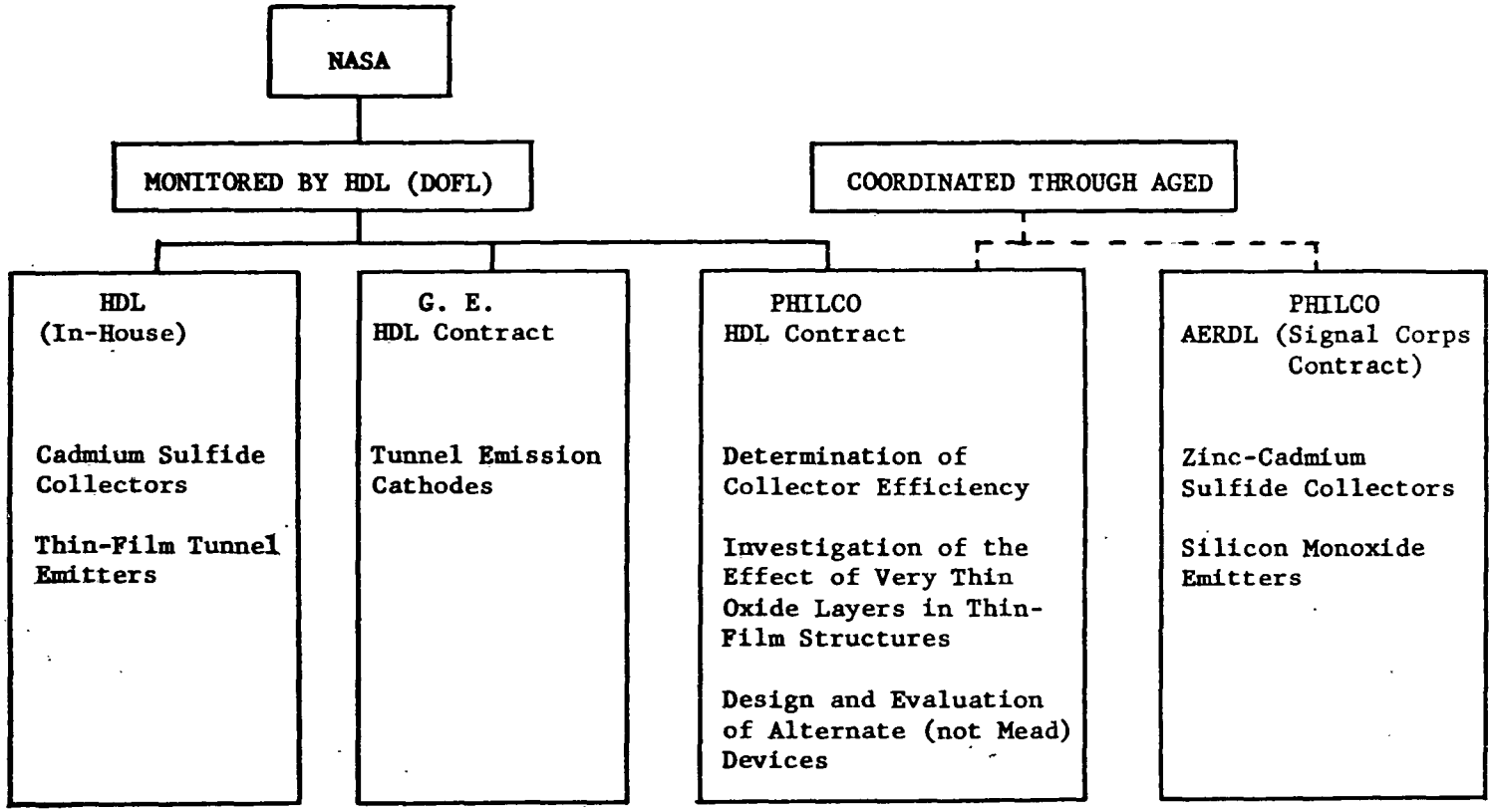

6. ACKNOWLEDGMENT

In addition to the principle authors, Q. C. Kaiser and G. G. Avis contributed to this report. Although not regularly assigned to this project, E. R. Fajardo rendered valuable engineering assistance in connection with the development of the multiple beam interferometer.

7. REFERENCES

(1) Kaiser, Q. C., Meyer, O. L., and Scales, J. L., DOFL Progress Report PR-61-12 "Radiation Resistant Electronics," p 10, 8 August 1961 to 31 December 1961.

(2) Murphy, E. L., and Good, R. H., Phys. Rev. 102, 1464 (1956).

(3) Holm, R., J. Appl. Phys. 22, 569 (1951).

(4) Schwarz, R. F., and Spratt, J. P., Proc. I.R.E. 50, 467 (1962).

(5) Kaiser, Q. C., Meyer, O. L., and Morris, H., DOFL Progress Report PR-62-4, "Radiation Resistant Electronics," p 42, 1 January 1962 to 30 June 1962.

(6) Kahng, D., Proc. I.R.E. 50, 1534 (1962).

(7) Kaiser, Q. C., Meyer, O. L., Morris, H., DOFL Progress Report PR-62-4, "Radiation Resistant Electronics," p 19, 1 January 1962 to June 1962.

(8) Wexler, A., and Hasegawa, S., J. Res. National Bureau of Standards, 53, 19 (1954).

(9) Harman, G. G., Higier, T., and Meyer, O. L., J. Appl. Phys. 33, 2206 (1962).

(10) Handy, R. M., Phys. Rev. 126, 1968 (1962).

(11) Fisher, J. C., and Giaever, I., J. Appl. Phys. 32, 172, (1961)

(12) Mead, C. A., Phys. Rev. 128, 2088 (1962).

(13) Carroll, P., Bul. Amer. Phys. Soc. Ser II 7, 432 (1962).

(14) Kaiser, Q. C., Meyer, O. L., and Morris, H., DOFL Progress Report PR-62-4, "Radiation Resistant Electronics," p 26, 1 January 1962 to 30 June 1962.

(15) Winterbottom, A. B., "Optical Studies of Metal Surfaces," DET KGL. Norske Videnskabers Selskabs Shrifter 1955 NR 1. Trondheim, 1955.

(16) Archer, R. J., J. Opt. Soc. Amer. 52, 970 (1962)

(17) Kaiser, Q. C., Meyer, O. L., and Morris, H., DOFL Progress Report PR-62-4, "Radiation Resistant Electronics," p 34, 1 January 1962 to 30 June 1962.

(18) ibid, p 36.

(19) Ruppel, I. W., and Smith, R. W., R.C.A. Rev. 20, 702 (1959).

(20) See for example, the series of papers appearing in The R.C.A. Review, September issue of Volume 12 (1951).

(21) See for example the entire December issue of the R.C.A. Review, Volume 20, (1959).

(22) Wright, G. T., J. Brit. I.R.E., 22, 337 (1960).

(23) Weimer, P. K., Proc. I.R.E., 50, 1462 (1962). See also NEREM Record (Boston, Mass, 1962).

(24) Tantraporn, W., Electronics 35, No. 12 29 (1962). See also Proc NEC 18, 736 (1962).

(25) Shockley, W., Proc. I.R.E., 40, 1365 (1952)

(26) van der Ziel, A., Proc I.R.E. 50, 1985 (1962)

(27) Kaiser, Q. C., Meyer, O. L., and Morris, H., DOFL Progress Report PR-62-4, "Radiation Resistant Electronics," p 42, 1 January 1962 to 30 June 1962.

(28) ibid, pp 14, 42.

DISTRIBUTION

National Aeronautics and Space Administration
Washington 25, D. C.
- Code FC/A. M. Andrus
- Code RET (3 copies)
- Code RP/W. C. Scott
- Code RV/J. W. Keller
- Code RTR/T. T. Neill
- Code MSA/M. J. Krasmian

National Aeronautics and Space Administration
Goddard Space Flight Center
Greenbelt, Maryland
- Attn: J. Purcell
- Attn: L. Winkler
- Attn: J. C. Lyons
- Attn: M. Maxwell
- Attn: R. Van Allen

National Aeronautics and Space Administration
Langley Research Center
Langley Air Force Base, Virginia
- Attn: J. Still
- Attn: C. Husson

National Aeronautics and Space Administration
George C. Marshall Space Flight Center
Huntsville, Alabama
- Attn: D. L. Anderson
- Attn: J. Kessel
- Attn: H. Brown
- Attn: T. Keeffe

National Aeronautics and Space Administration
Manned Spacecraft Center
P. O. Box 1537
Houston 1, Texas
- Attn: Instrumentation and Electronic Systems Division
- Attn: R. Sawyer
- Attn: D. M. Hickman

Jet Propulsion Laboratory
4800 Oak Grove Drive
Pasadena 3, California
- Attn: F. Goddard
- Attn: J. Konkel
- Attn: J. D. Allen

National Aeronautics and Space Administration
Lewis Research Center
21000 Brookpark Road
Cleveland 35, Ohio

National Aeronautics and Space Administration
Ames Research Center
Moffett Field, California

National Aeronautics and Space Administration
Flight Research Center
P. O. Box 273
Edwards, California
Attn: T. W. Eisenman

Department of the Navy
Bureau of Naval Weapons
Washington 25, D. C.
Attn: B. Weiner, Code RAAV-110

Department of Defense
Director of Defense Research and Engineering
Washington 25, D. C.
Attn: J. Grodsky

Internal

Horton, B. M./McEvoy, R. W., Lt. Col
Apstein, M./Guarino, P. A./Gerwin, J. L.
Kalmus, H. P./Spates, J. E./Schwenk, C. C.
Rotkin, I./Godfrey, T. B./Eichberg, R. L.
Bryant, W. T./Distad, M. F./McCoskey, R. E./Moorhead, J. G.
Hardin, C. D., Lab 100
Sommer, H., Lab 200
Hatcher, R. D., Lab 300
Hoff, R. S., Lab 400
Nilson, H. M., Lab 500
Flyer, I. N., Lab 600
Campagna, J. H., Div 700
DeMasi, R., Div 800
Landis, P. E., Lab 900
Tozzi, L. M., 210
Haas, P., 230
Peperone, S. J., 240
Witte, J. J., 250
Seaton, J. W., 260
Kirshner, J. M., 310
Harris, F. T., 320
Kurkjian, B., 330
Cullinane, J. J., 410

Fisher, E. D., 430
Fraumann, J. W., 440
Piper, W. M., 450
Taft, S. C., 510
Johnson, R. N., 520
Tuccinardi, T. E., 530
Mead, O. J., 610
Moore, W. J., 620
Marshburn, C. E., 630
Walsh, G. W., 640
Geist, S. M., 710
Keehn, G. R., 710
Grautoff, W. B., 720
Menapace, H. V., 730
Price, H. W., Jr., 750
Pratt, H. A., 800
Reznik, B., 850
Benderly, A. A., 910
Avis, G. G., 910
Kaiser, Q. C., 920 (5 copies)
Klute, C. H., 920 (10 copies)
Anstead, R. J., 920
Doctor, N. J., 920
Meyer, O. L., 920 (5 copies)
Morris, H., 920 (5 copies)
Scales, J. L., 920 (5 copies)
Stinchfield, J. M., 920
Wetzel, G. B., 920
Van Trump, J. H., 930
Chandler, H. G., 930
Otley, K. O., 930
Reddan, M. J., 930
Ward, A. L., 930
Isler, W. E., 910
Goodrich, R. B., 940
Technical Reports Unit, 800
Technical Information Office, 010 (10 copies)
HDL Library (5 copies)